Crystallized phases: induced index change

Phase	PDF #	System	Group	a(Å)	b(Å)	c(Å)
NaF	36-1455	Cubic	Fm3m	4.633	4.633	4.633
NaBr	36-1456	Cubic	Fm3m	5.974	5.974	5.974
NaBr	27-0658	Cubic	N/A	12.133	12.133	12.133
Ag	04-0783	Cubic	Fm3m	4.086	4.086	4.086
Ag	41-1402	Hexagonal	P63/mmc	2.886	2.886	10.000
AgF	25-0762	Cubic	Pm3m	2.945	2.945	2.945
AgF	03-0890	Cubic	Fm3m	4.921	4.921	4.921
AgF	32-1004	Hexagonal	P63mc	3.246	3.246	6.226
AgF_2	19-1134	Orthorhombic	N/A	5.813	5.529	5.073
AgF_3	45-0159	Hexagonal	N/A	8.989	8.989	9.815
AgBr	06-0438	Cubic	Fm3m	5.774	5.774	5.774

XRD pattern of virgin and crystallized PTR

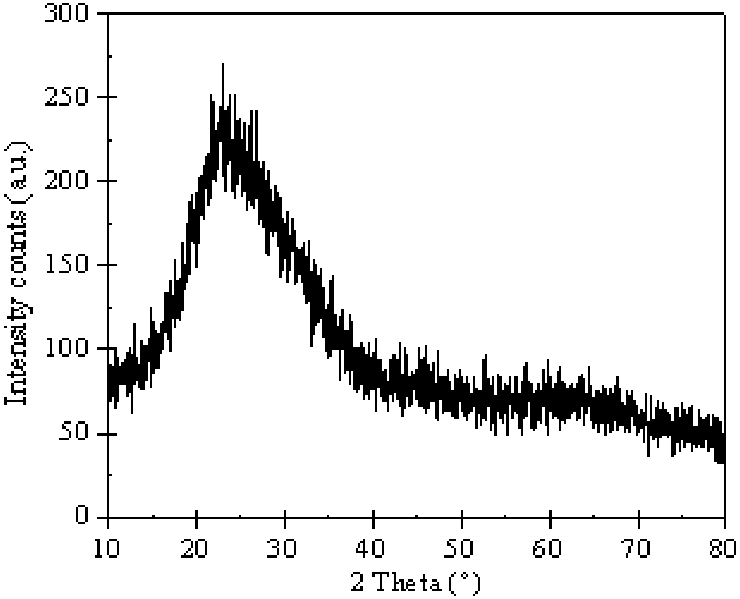

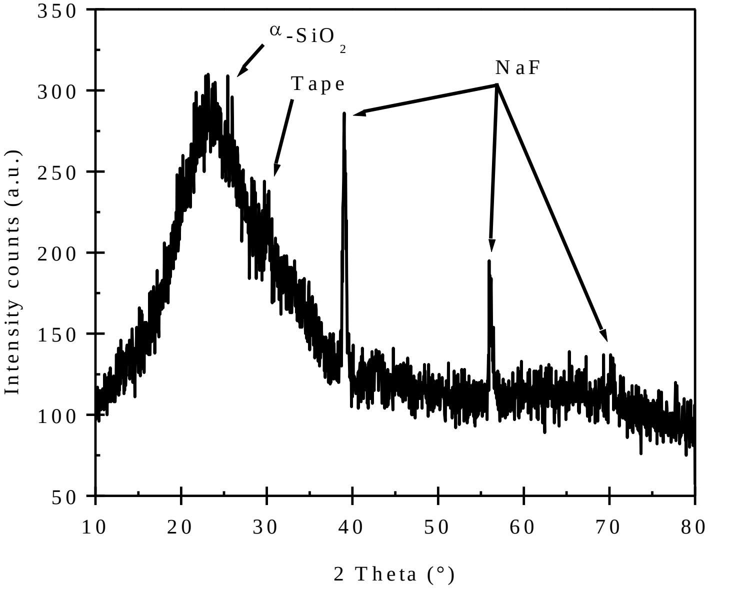

(A-B) Low- and (C-D) High-magnification TEM images of spontaneously crystallized PTR glass prepared by TP and FIB respectively.

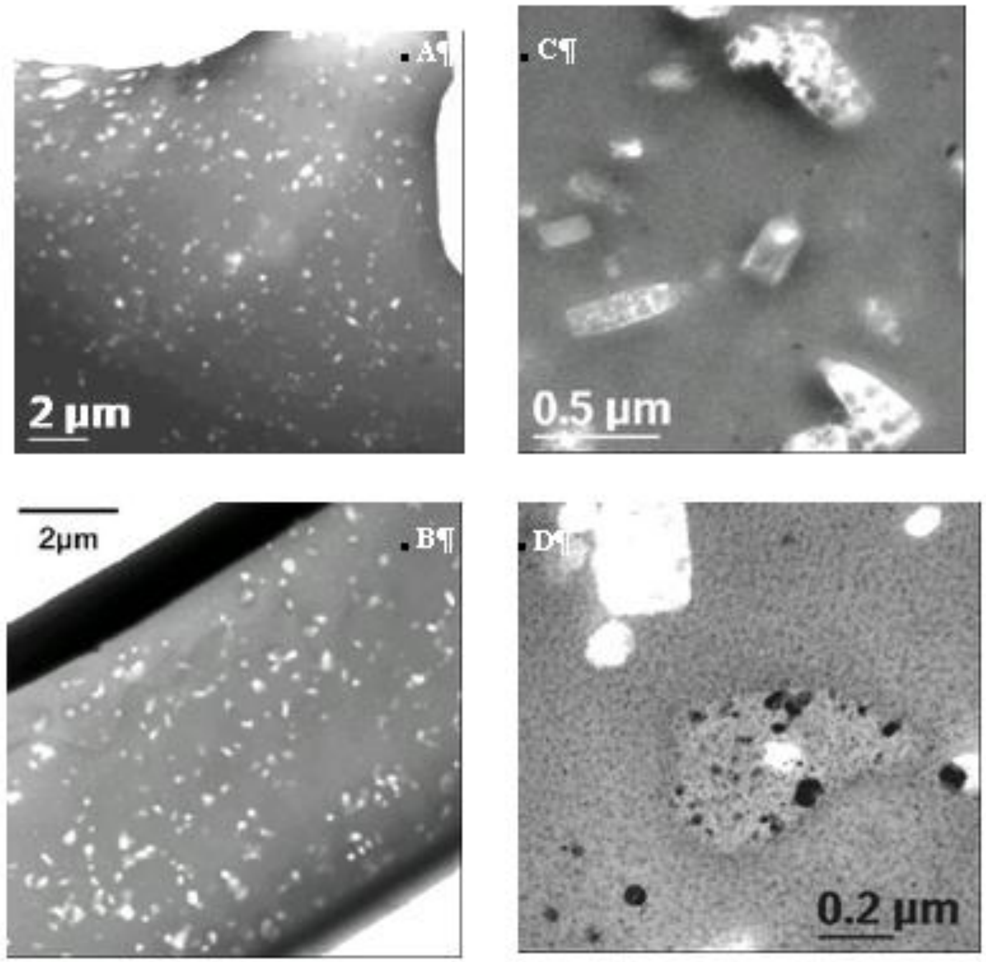

Photosensitivity (PS)

permanent
refractive index change Δn
by laser exposure

points of views

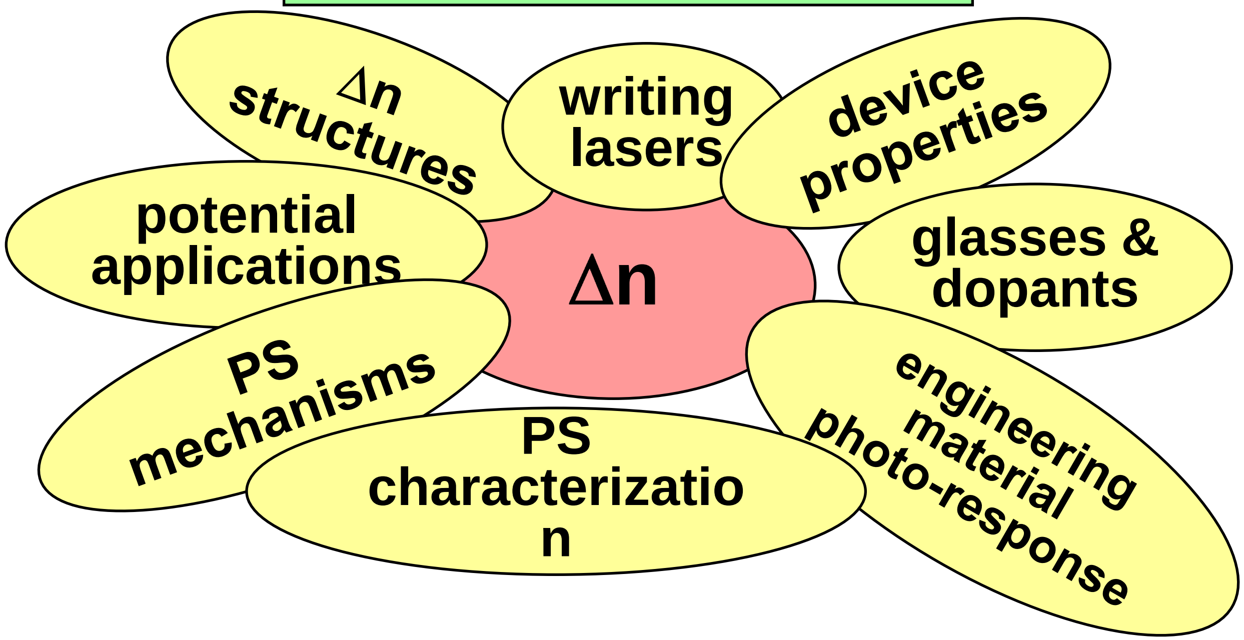

From "Photosensitity, Fundamentals and Overview", H. Ebendorff-Heidepriem

Laser material modification: pulsed direct write or cw laser interaction, ablation

- ***Focusing a cw source or a femtosecond near-IR beam in a transparent material produces a local change of the refractive index***
- ***fs-regime writing allows volumetric processing and minimizes thermally induced defects often seen in ns experiments; lack of thermal "damage" to material results in clean features***
  - ***Glass structure reorganization (bond bending and/or breaking)***
  - ***Photoexpansion or densification***
  - ***Refractive index modification (+ or -)***
- ***Sub-micron precision 0.5 μm demonstrated for fs (Schaffer et al., Opt. Lett. 26, 2001)***
- ***Real time serial fabrication, 3-D structuring possible, not amenable to high volume processing due to limitations of writing speed***

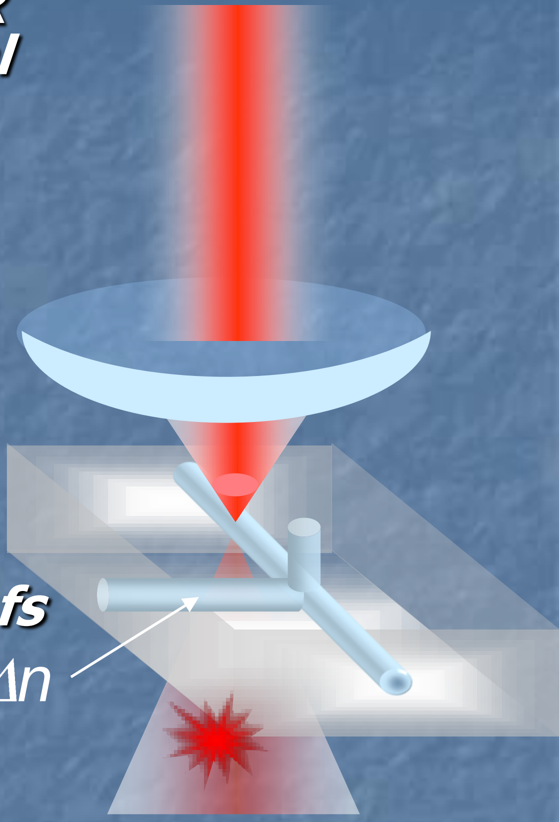

ns or other "conventional" exposure

fs exposure with minimal debris and thermal

Examples of Processing of Glass and Ceramic Materials

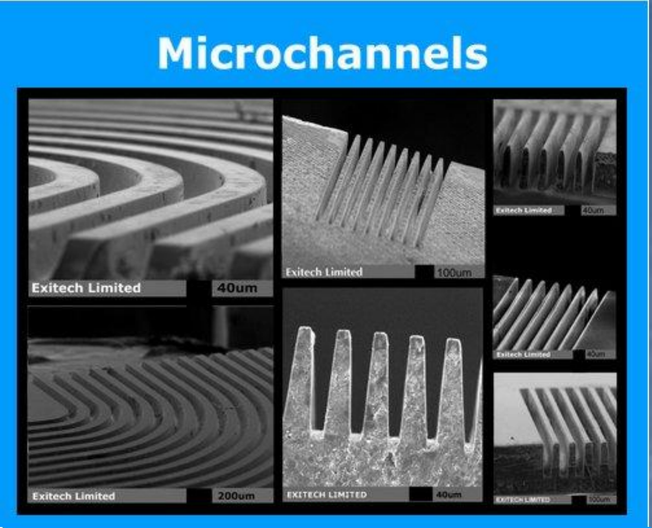

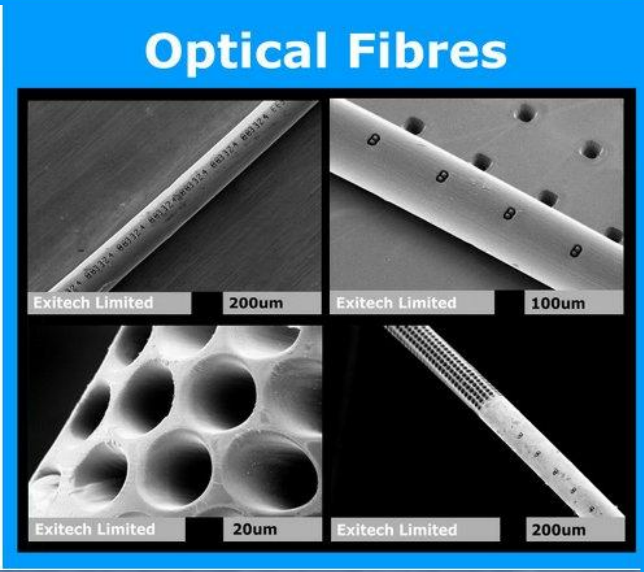

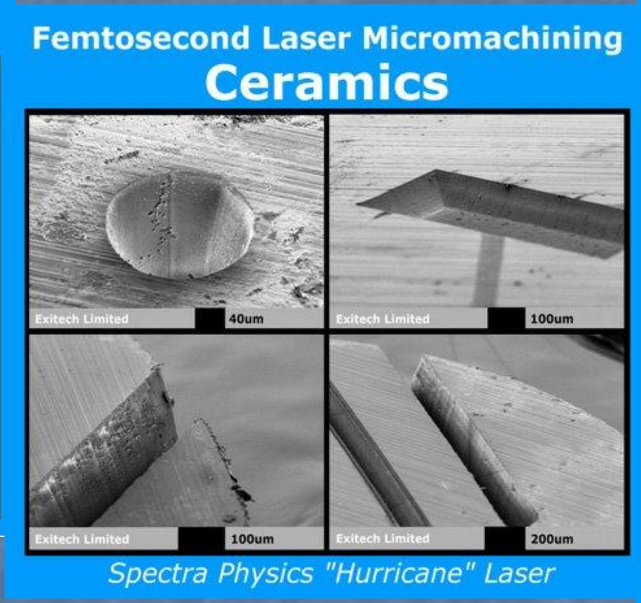

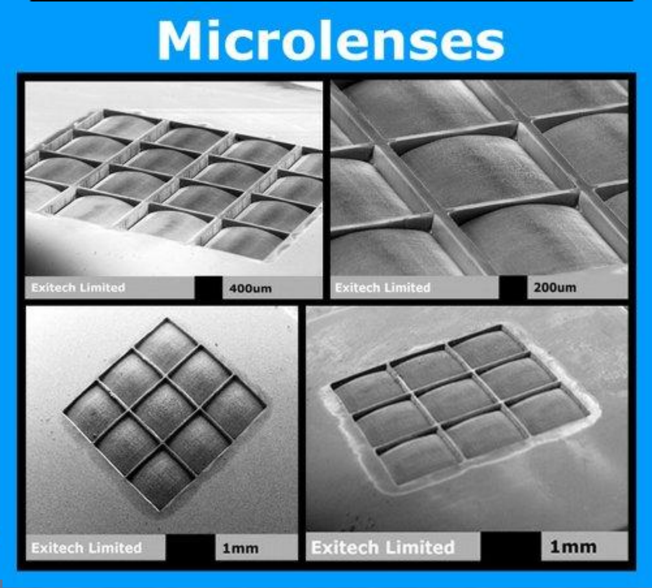

Courtesy Exitech Corp.

Really Need True 3D Patterns and a Cost Effective Processing Approach

Two regimes of *direct* writing

Dependence of axial shape of structural modification on writing approach

transverse writing

longitudinal writing

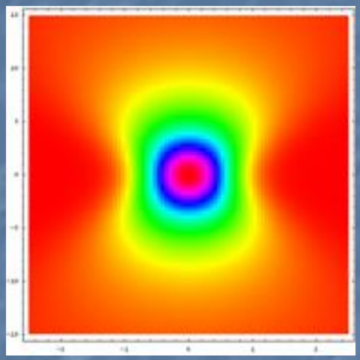

1-photon

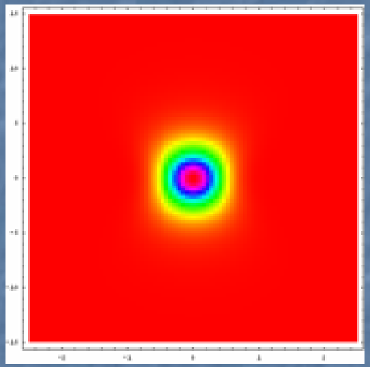

2-photon

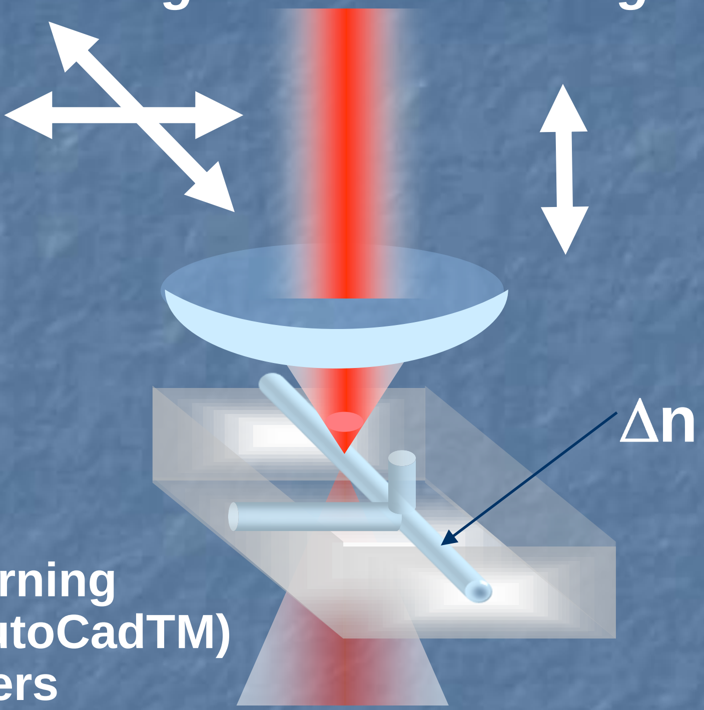

THE AEROSPACE CORPORATION

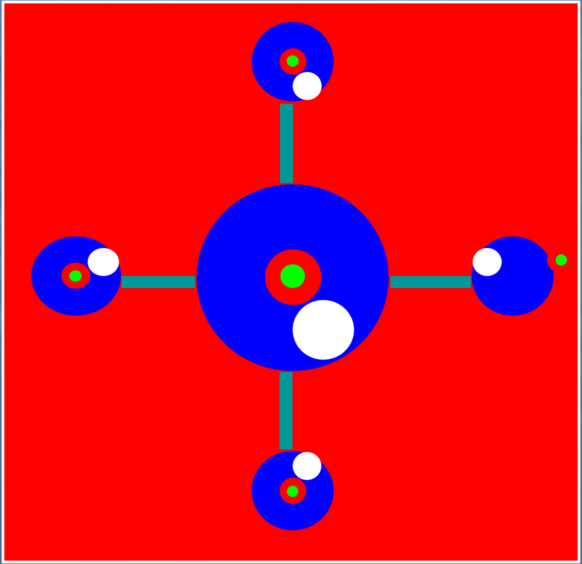

Direct-Write Patterning Using Various CAD (AutoCadTM) Patterning Layers

- **355 nm**
- **266 nm (high dose)**
- **266 nm (low dose)**
- **248 nm**

Additional "Layers" that can be added

- Platinum metal deposition
- Imbedded exposure

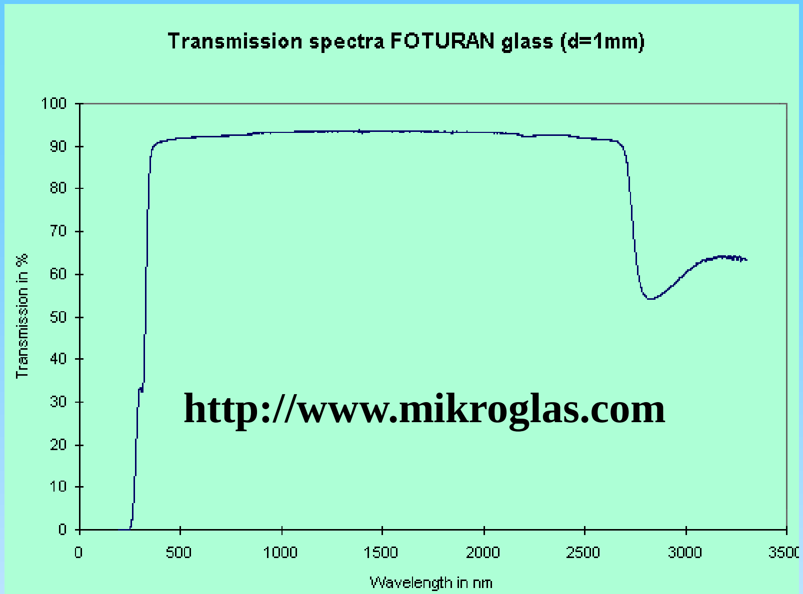

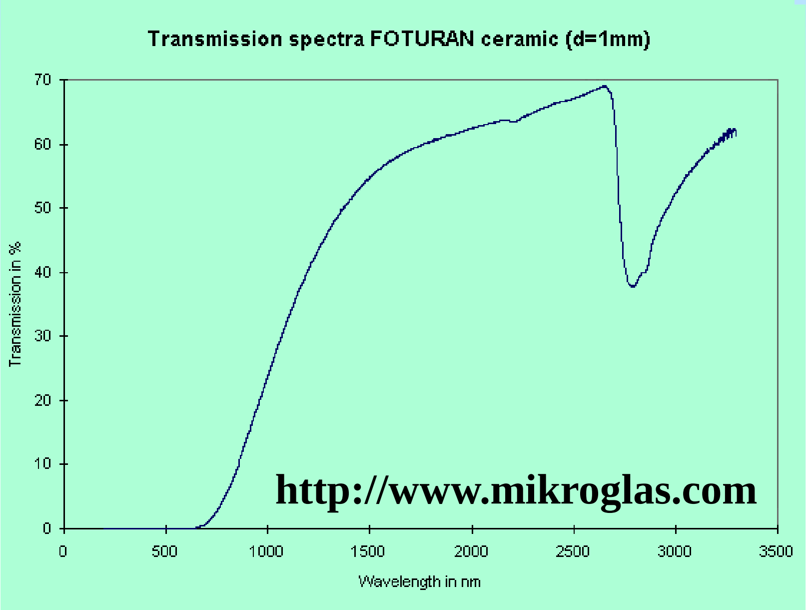

What is a Photostructurable Glass Ceramic Material or Photoceram

Example: Foturan^{TM} (Schott Corp.)

Property	Foturan in the Vitreous State
Young's Modulus	78 x 10^3 N/mm^2
Poisson's Ratio	0.22
Knoop Hardness	4600 N/mm^2
Modulus of Rupture (MOR)	60 N/mm^2
Density	2.37 g/cm^3
Thermal Expansion	8.6 10^{-6}/K
Thermal Conductivity	1.35 W/mK @ 20^{o}C
Specific Heat	0.88 J/gK @ 25^{o}C
Glass-ceramic Transformation Temperature	465 ^{o}C
Electrical Conductivity	8.1x 10^{12} Ohm-cm @ 25^{o}C 1.3 x 10^7 Ohm-cm @ 200^{o}C
Dielectric Constant	6.5 @ 1MHz, 25^{o}C

Schott/SGT April 2002

Copyright © 2002 by The Aerospace Corporation

THE AEROSPACE CORPORATION

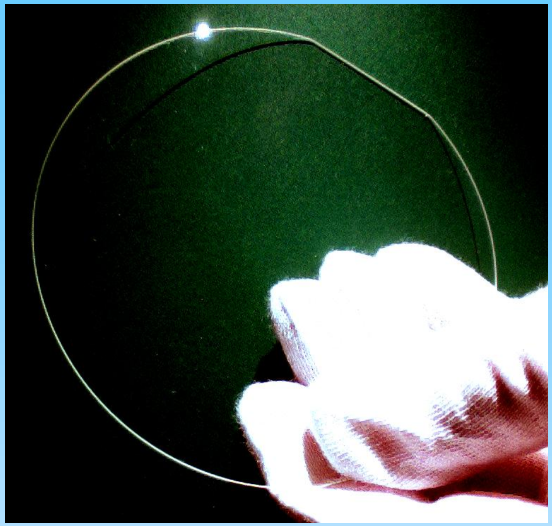

Processing Photoceramic Glasses

Typical Process Flow

Step 1: Illumination/Latent Image

$$Ce^{3+} + h\nu\ (312\text{nm}, 2\ \text{J/cm}^2) \rightarrow Ce^{4+} + e^-$$

$$e^- + Ag^+ \rightarrow Ag^0$$

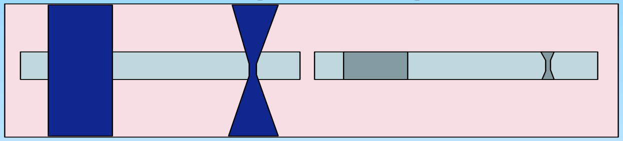

Step 2: Ceramization to a Meta-Silicate

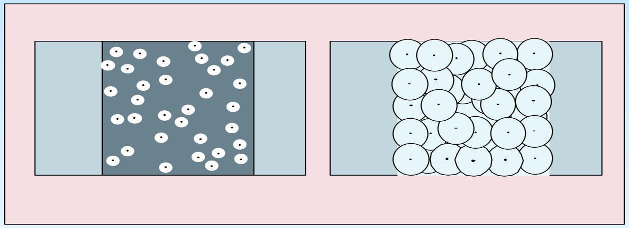

Step 3: Preferential Isotropic Etching

- Crystalline Li_2SiO_3 dissolves 20x faster than the amorphous glass in 5% hydrofluoric acid.
- $Li_2SiO_3 + 3HF \rightarrow 2LiF + H_2SiF_6 + 3\ H_2O$

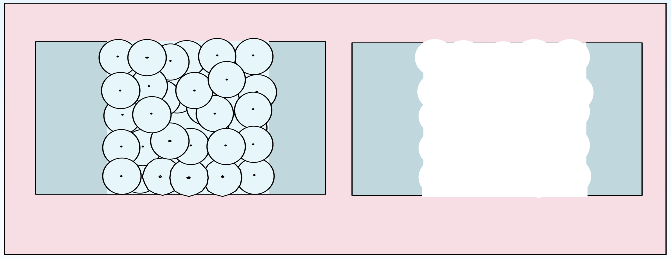

Schott/SGT April 2002

Copyright © 2002 by The Aerospace Corporation

THE AEROSPACE CORPORATION

Exposure at Multiple Wavelengths Can Result in the Fabrication of Unique 3D Patterns

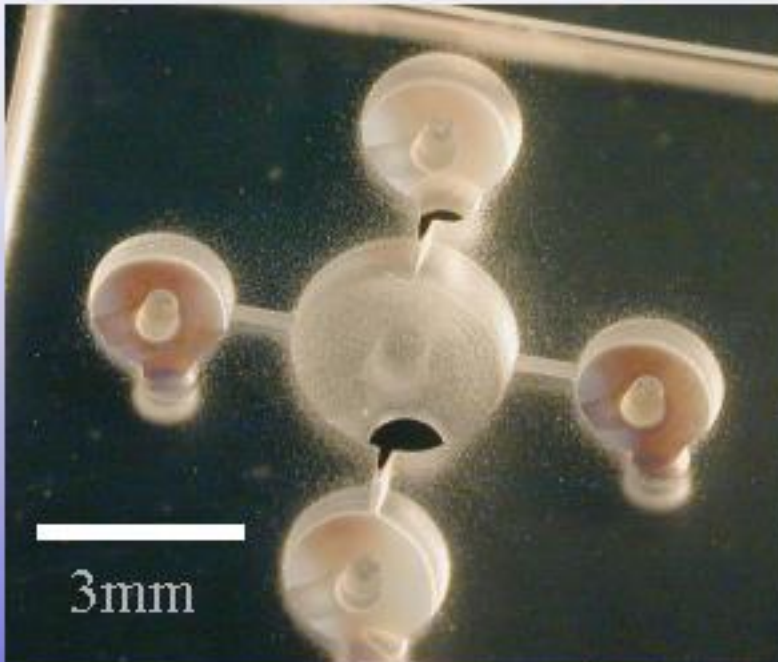

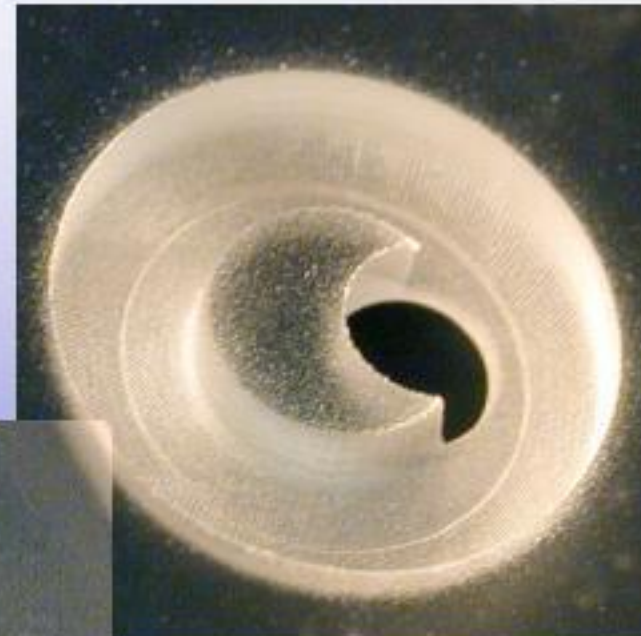

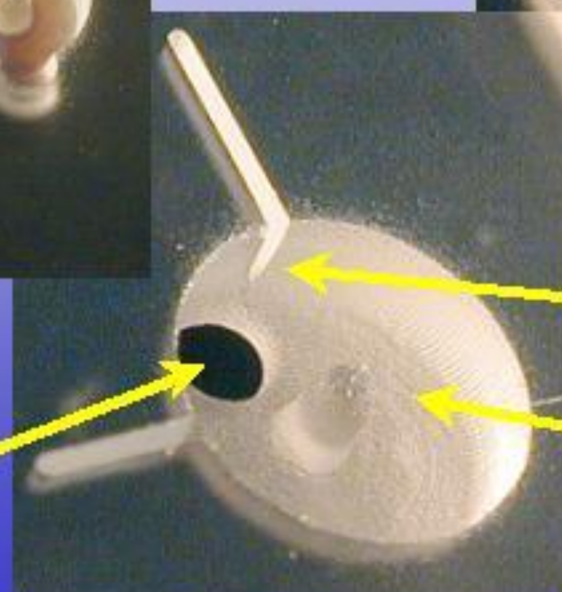

Via hole through 1mm thick wafer @355nm

500 microns deep @248 nm

700 microns deep @266nm

So…as we'd expect

- Chemistry dictates the structure of the material (purity matters)
- Structure dictates the properties
- Optical properties are dictated by chemistry and processing route (thermal history dictates V, ρ => n); impurities define intrinsic absorption properties (α, α_2)
- Thus…material's photo-response will be dependent on all of these attributes

What does this mean to absorption? network formers and modifiers

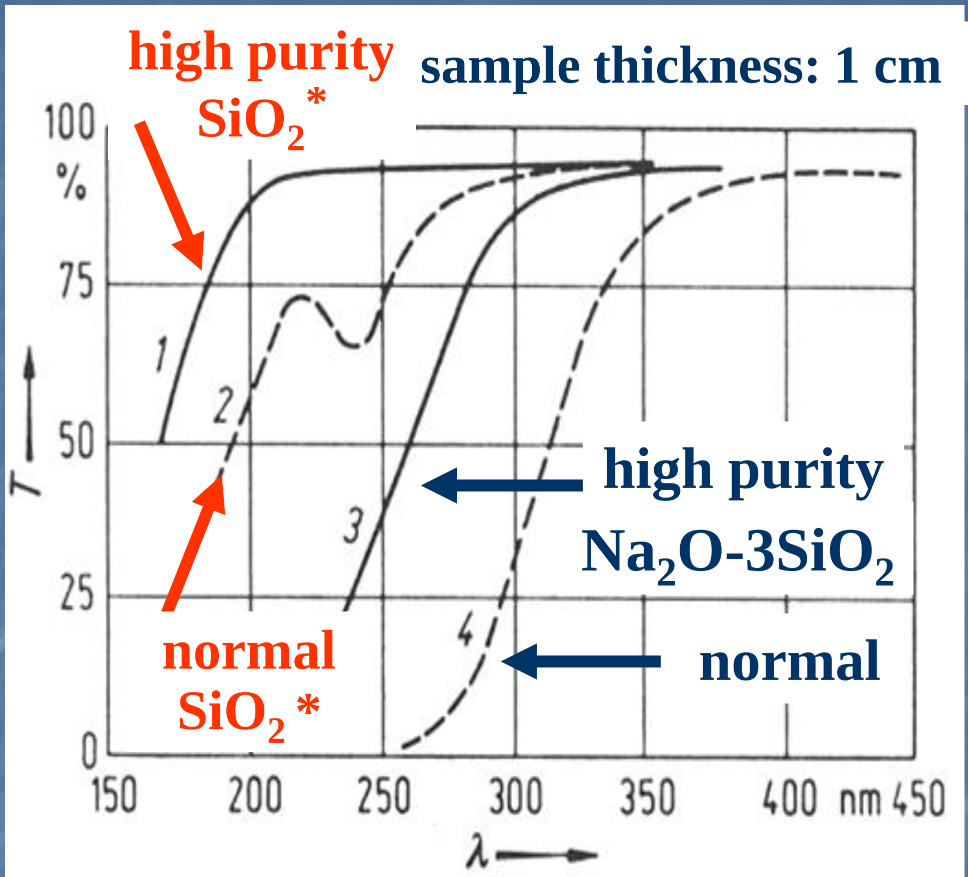

- Additions of Al_2O3 and B_2O_3 improve the tetrahedral network structure, consuming NBO's and move the UV edge back up to higher frequencies.
- PbO which is present in moderate concentrations in may flint optical glasses, shifts (ν) the UV edge significantly.

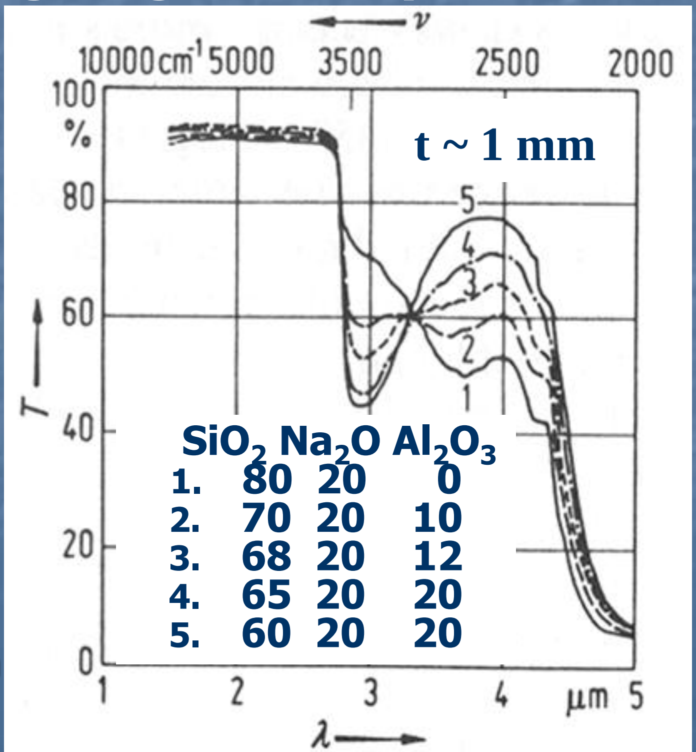

- **Network:** SiO_2 **Modifier**: 25 mol% Na_2O

* BO: O-Si-O (covalent)

- Formation of NBO with alkali addition

NBO: Si-O⁻ Na⁺ (ionic-like)

- Lower BE electrons (red) shift UV edge

higher field strength ions shift less

Li<Na<K, etc.

- Impurities: Fe, Mn, etc.

Absorption and Dispersion

Network	UV edge position	

- SiO_2 glass 155-160 nm (7.8 eV)
- GeO_2 glass 200 nm (6.2 eV)
- B_2O_3 glass 172 nm (7.2 eV)
- P_2O_5 glass 145 nm (8.6 eV)
  - P_2O_5 has a tetrahedral structure with a double-bonded oxygen
- Al_2O_3 sapphire (single crystal, annealed film)
  - sc 145 nm (8.55 eV)
  - film 182 nm (6.8 eV)

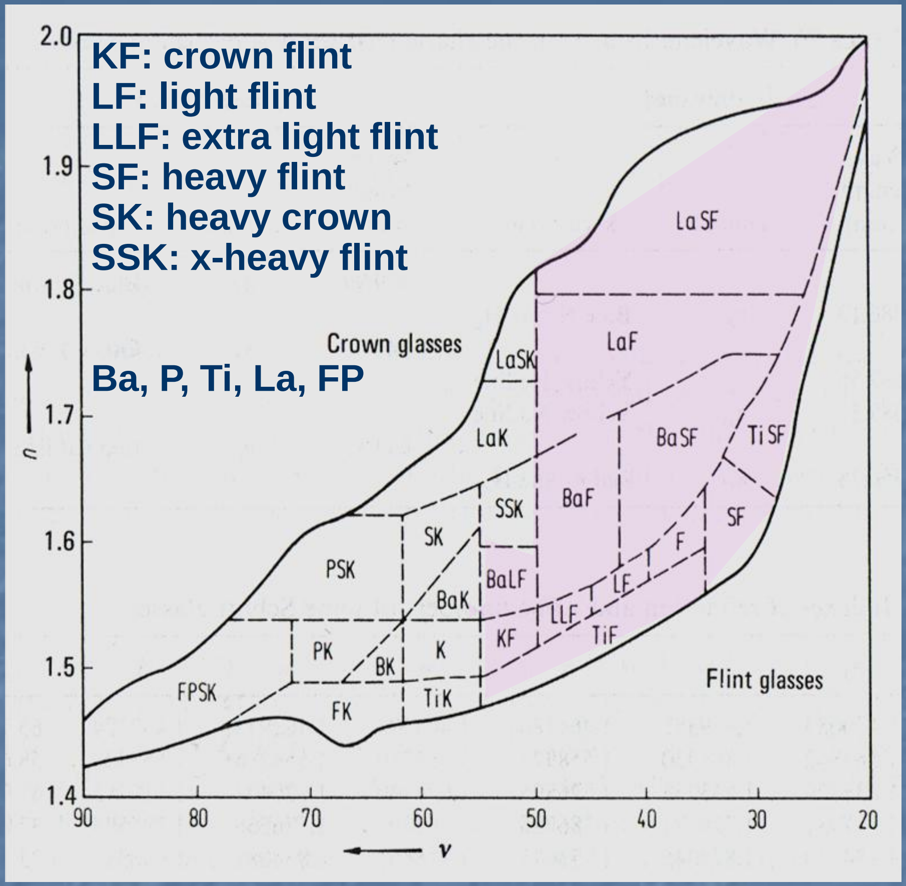

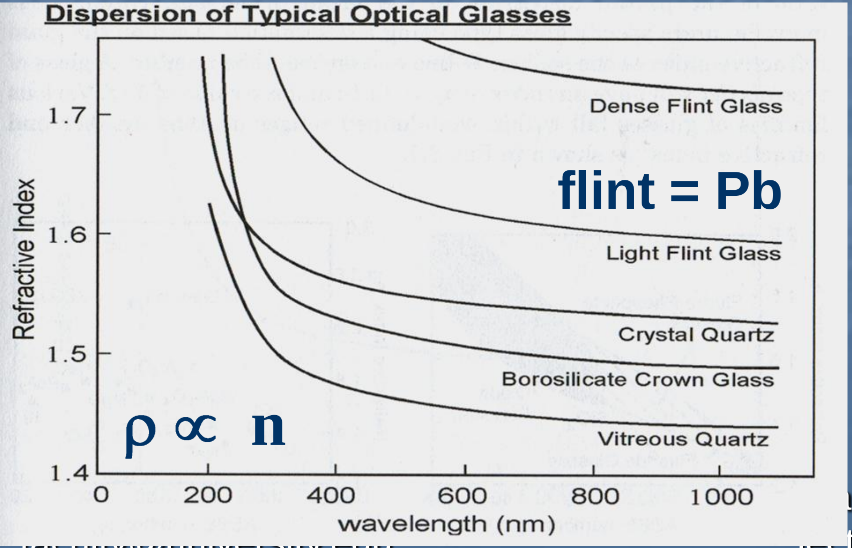

Li_2O-SiO_2 glass 188 nm (6.6 eV)

➔ Foturan: Ce, Al_2O_3, Ag, Zn, Sn

Na_2O-SiO_2 glass 207 nm (6.0 eV)

K_2O-SiO_2 glass 214 nm (5.8 eV)

from "Optical Materials," J.H. Simmons, K.S. Potter (Academic Press) NY (2001); "Glass" H. Scholze, Springer (1991)

Photo-induced property changes

- Exposure ($h\nu$) induced:
  - Structural reorganization (bond bending); *reversible* As_2S_3
  - Structural reorganization (bond breaking) *permanent* As_2S_3 and other glasses
  - Structural reorganization (melting and solidification: cooling rate causes ΔV, Δn)
  - Crystallization - realized through exposure and heat treatment=> to yield new phase with:
    - Refractive index variation (Δn crystal $\neq \Delta n$ glass) PTR
    - Creation of a new phase with etch rate (contrast) different than glass Foturan

Material absorption: response to laser light network structure, dopants

Material absorption spectra

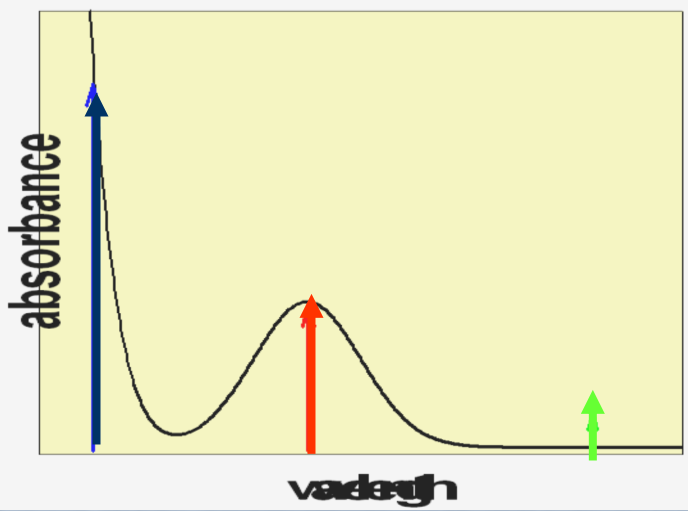

spectral range	wave-length	laser type	Regime
VUV	157nm	F_2	pulsed
UV	193nm	ArF excimer	pulsed
	244nm	Ar^+ 2.Harmonic	cw
	248nm	KrF excimer	pulsed
	266nm	Nd:YAG 3.Harm.	pulsed
	325nm	HeCd	cw
VIS	457 – 488nm	Ar^+ various lines	cw
NIR	800nm	Ti:sapphire	fs

UV-Edge

Excitation: $\lambda_{edge} \leq \lambda_{Laser}$

λ_{glass} *band-gap*

$Ge\text{-}SiO_2$	157nm
$PbO\text{-}SiO_2$	244 & 266nm
Zr-Ba-F	193 nm
Ga-La-S	244 nm
As-S	550 nm

Defect, Dopant

absorption

$\lambda_{defect,dopant} \approx \lambda_{Laser}$

selective excitation

$Ge\text{-}SiO_2$	244 & 248 nm
Eu^{2+}, Ce^{3+}	244 & 248 nm
Eu^{3+}	466 nm
Ag^+	420 nm

Laser (writing) wavelength

λ_{laser} » λ_{glass}

Single vs multi-photon processes

glass	800 nm
$Ge\text{-}SiO_2$	488nm

From “Progress in Photosensitivity Fundamentals and Overview,” Heike Ebendorff-Heidepriem, Proc. 1st International Workshop on Glass and the Photonics Revolution (2002)

Dopants/impurities and spectral regimes

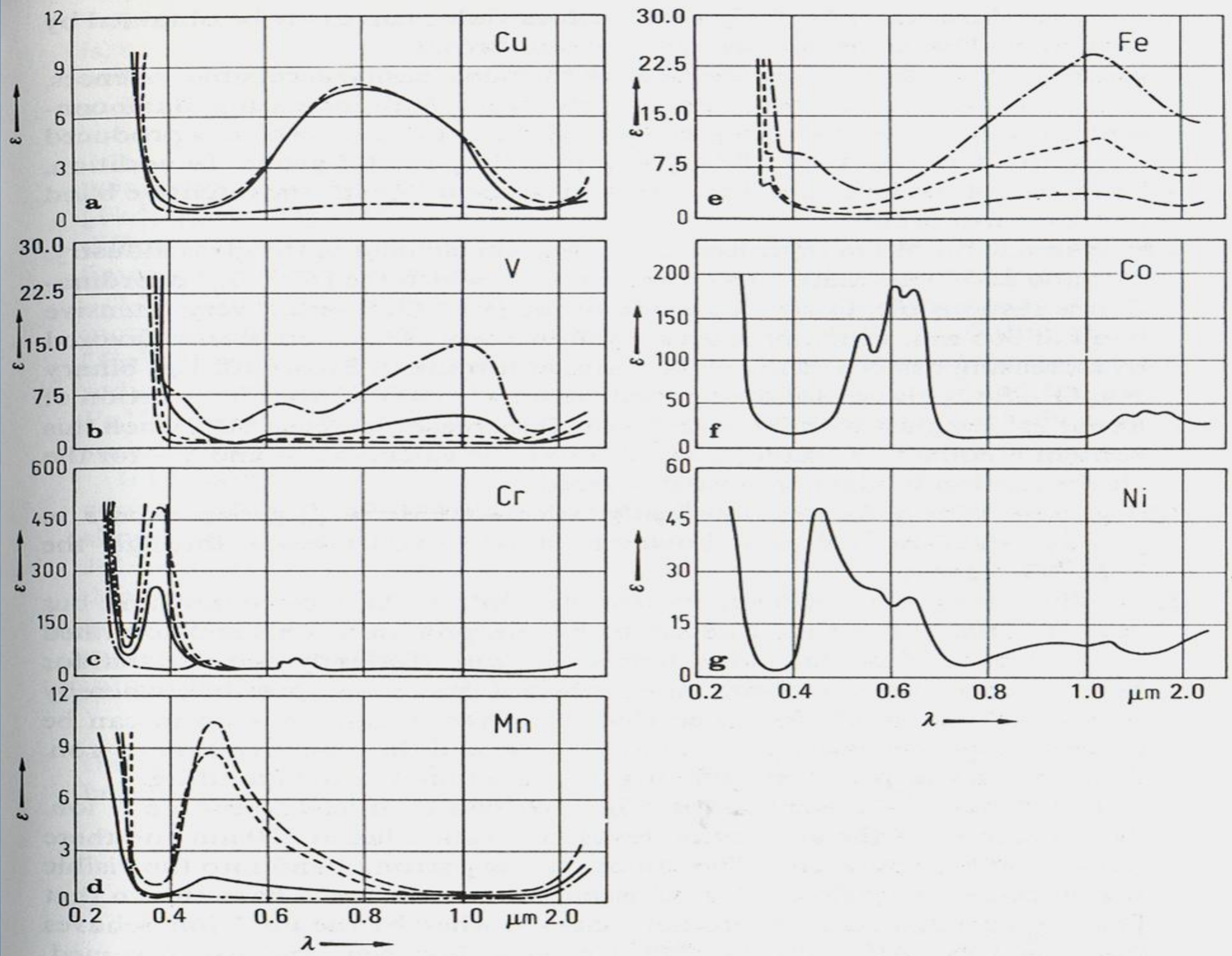

FIGURE 109a–g. Spectra of some transition elements in sodium silicate glasses, from Bamford [41, 42] (ε = molar normal extinction coefficient in 1/[mole cm]).

——— Na_2O content about 15 mole % } Melted in oxidizing atmosphere
— — — Na_2O content about 40 mole %

—·— Na_2O content about 15 mole % } Melted in reducing atmosphere
- - - - - Na_2O content about 40 mole %

Now…what happens upon exposure to light?

- Absorption and other properties of material
- Form of the material (bulk, film, fiber)
- Desired modification we want
- Exposure conditions
  - Permanent, reversible, ablative

Glass ⇔ Laser

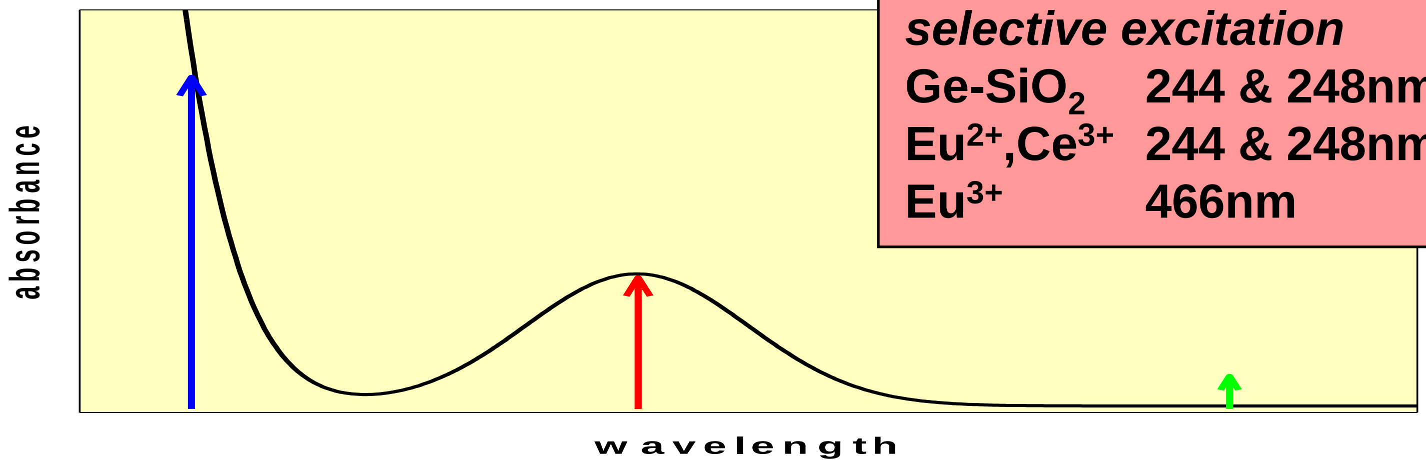

Defect, Dopant

$\lambda_{defect,dopant} \approx \lambda_{Laser}$

selective excitation

$Ge\text{-}SiO_2$	**244 & 248nm**
Eu^{2+}, Ce^{3+}	**244 & 248nm**
Eu^{3+}	**466nm**

Transmission-Edge

$\lambda_{edge} \geq \lambda_{Laser}$

band-gap, strong absorption

$Ge\text{-}SiO_2$	**157nm**
$PbO\text{-}SiO_2$	**244 & 266nm**
Zr-Ba-F	**193nm**
Ga-La-S	**244nm**

High Transmission

$\lambda_{glass} \gg \lambda_{Laser}$

nonlinear absorption

glass	**800nm fs**
$Ge\text{-}SiO_2$	**488nm**

Δn structures

- **grating: Δn modulation**
  - **Bragg gratings:** $\Lambda \geq 1\ \mu m$
  - **Long period gratings:** Λ = several 100 µm

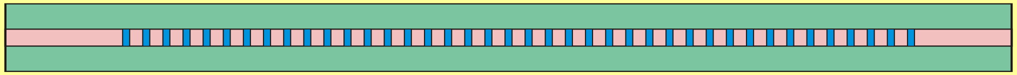

- **waveguides: Δn constant in 1D**

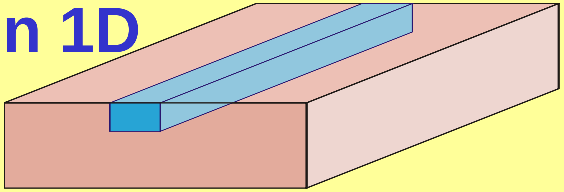

- **combination**
  1. **waveguide**
  2. **Bragg grating**

- **uniform exposure: Δn constant**

  → **PS characterisation**

Two distinct processing regimes of fs exposure: As_2S_3 films

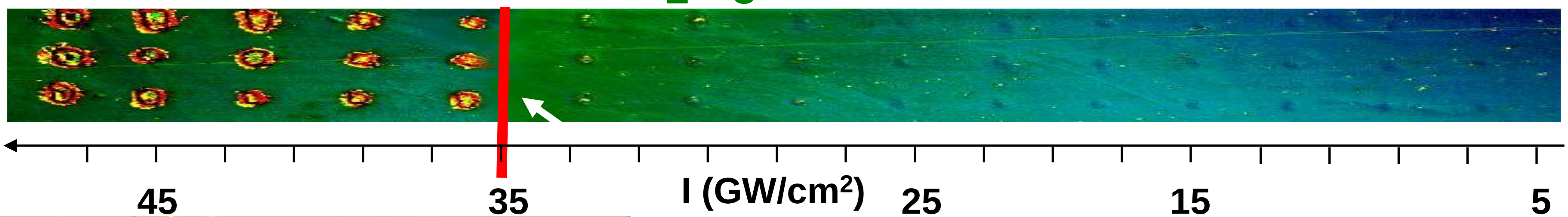

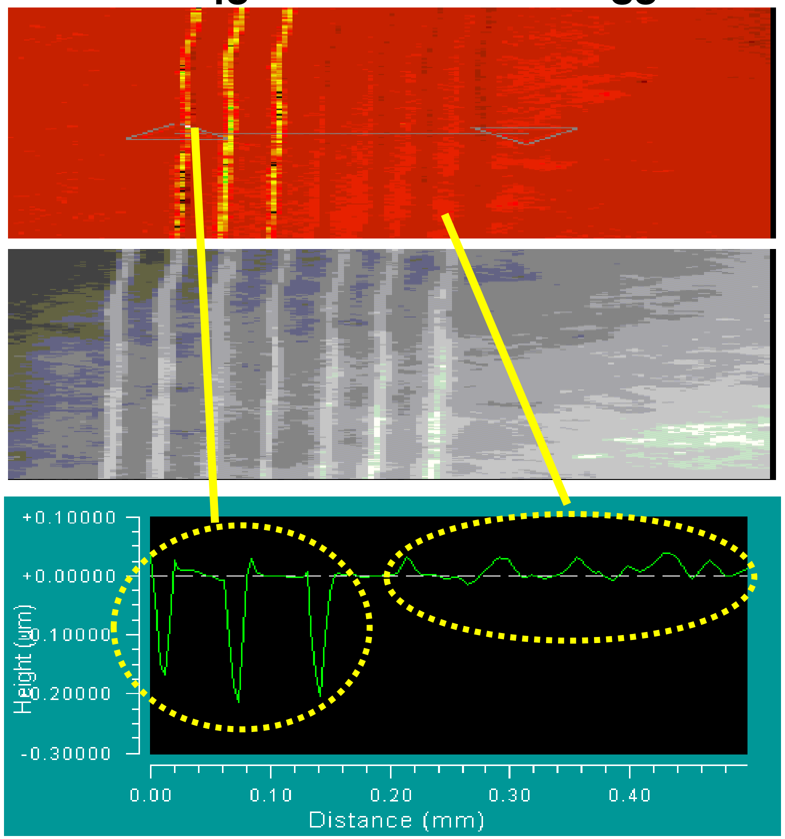

Deterministic ablation threshold ~35 GW/cm² for chalcogenides;

Absolute value varies with composition

<u>Trenches</u> (left) ablated through the chalcogenide thin film in ablative regime (I > 35 GW/cm²)

<u>Surface expansion</u> (right) realized in fs sub-threshold regime; <u>extent of change</u> in structure, topography and resulting index change is dependent on writing conditions and wavelength

"Direct femtosecond laser writing of optical waveguides in As_2S_3 thin films," A. Zoubir, M. Richardson, C. Rivero, A. Schulte, C. Lopez, K. Richardson, <u>Optics Letters</u> 29 7 (2004)

Direct write fs laser micro-fabrication in As_2S_3

Micro-ablation of relief features (grating)

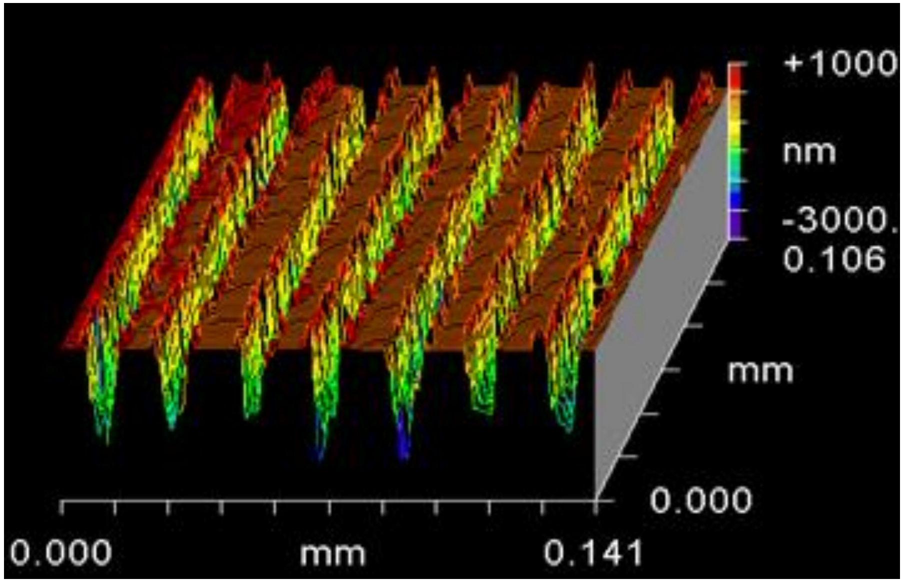

Micro-restructuring of material Photo-induced expansion (phase grating)

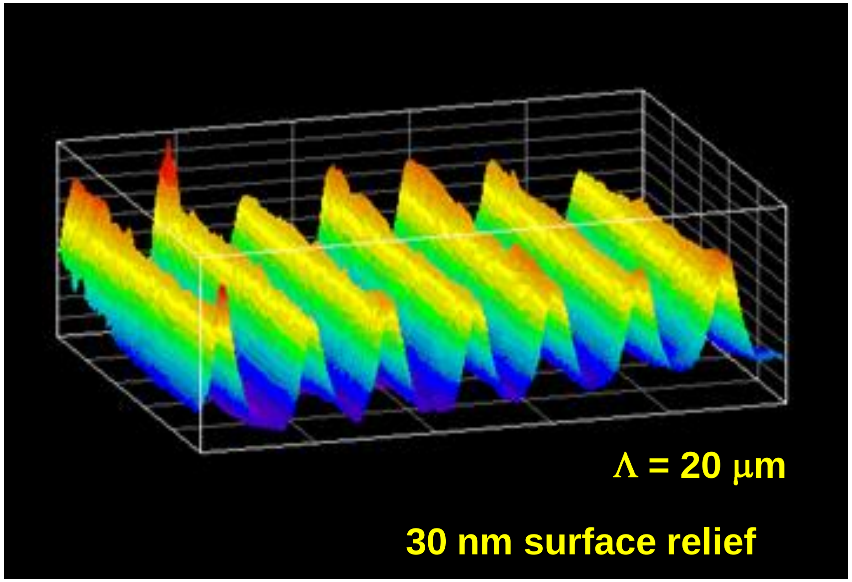

- **Surface profile (Zygo New View white light interferometer microscope)**
- **Typical width of exposure features ~10 µm (FWHM)**

"Microfabrication of waveguides and gratings in chalcogenide thin films," A. Zoubir et al., Technical Digest. CLEO pp 125-126 (2002)
"Direct femtosecond laser writing of optical waveguides in As_2S_3 thin films," A. Zoubir, M. Richardson, C. Rivero, A. Schulte, C. Lopez, K. Richardson, <u>Optics Letters</u> 29 7 (2004)

Design and Dimensions

Δn structure		starting device	
Bragg gratings			
1D	Fiber Bragg gratings	1D	single-mode fibre
			channel waveguide in planar device
2D	planar gratings	2D	thin film on substrate
	grating limited to exposed surface	3D	bulk
3D	volume gratings, holograms	3D	bulk: d = 2 - 7 mm d = 100-200µm
Long period gratings			
1D	LPG in fibre	1D	single-mode fibre
Waveguides			
1D	channel	2D	thin film on substrate
		3D	bulk: $E_{laser} > E_{band\text{-}gap}$
>1D	multi-mode	3D	bulk: $E_{laser} < E_{band\text{-}gap}$

Fabrications of Gratings

internal (longitudinal)

***self-written* due to standing wave interference**

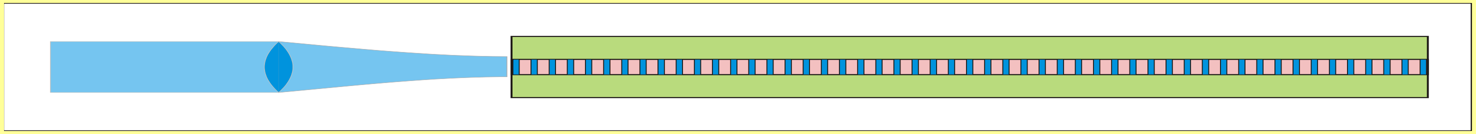

external

interferometric, phase-mask, point-by-point

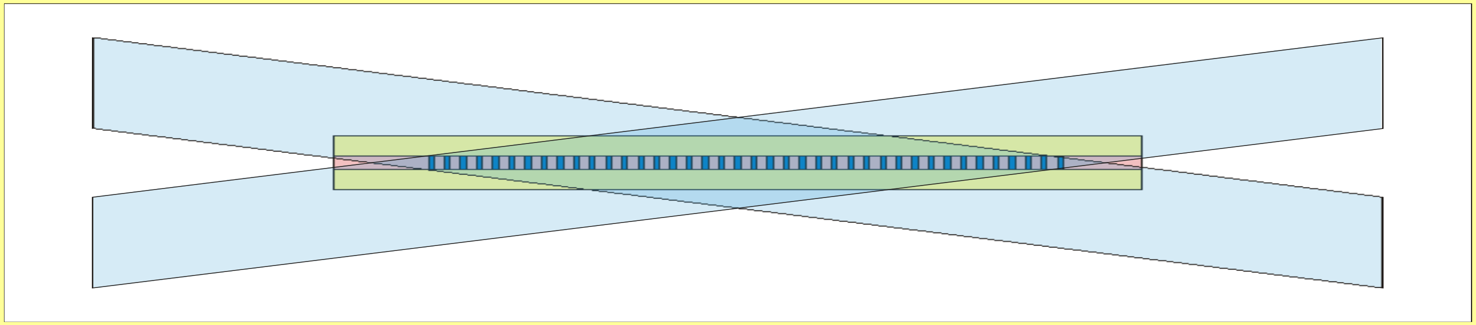

Glasses for Gratings

silica-based $\Delta n=10^{-5\ldots3}$

- **fibers, thin films $\rightarrow$ 1D or 2D gratings**
- **Ge-SiO_2: GODC @ 240nm**
  codopants: B,Sn ☺ / P ☹
- **Al-SiO_2: RE(Ce) doped**
- **P- SiO_2: Sn dopant**
- **H_2 treatment $\rightarrow$ PS increase**

heavy metal fluoride $\Delta n=10^{-5\ldots4}$

- **undoped, λ_w=193nm $\rightarrow$ 2D abs.-limited**
- **Ce^{3+},Eu^{2+} $\rightarrow$ fibres, thin film**

oxide(Si,B,P,Ge):Eu^{3+} $\Delta n=10^{-6\ldots5}$

- **volume gratings by 466nm-laser**

heavy metal oxide $\Delta n=10^{-2}$

- **PbO-SiO_2, λ_w=UV, bulk $\rightarrow$ 2D abs.-limited**
- **PbO-GeO_2, λ_w=UV, thin film $\rightarrow$ 2D**

Na-silicate/phosphate $\Delta n=10^{-?}$

- **ion-exchange $\rightarrow$ wg $\rightarrow$ 1D or 2D grating**

Fiber Bragg Gratings

uniform

const. grating period Λ
const. Δn_{mod} amplitude
phase fronts perpendicular

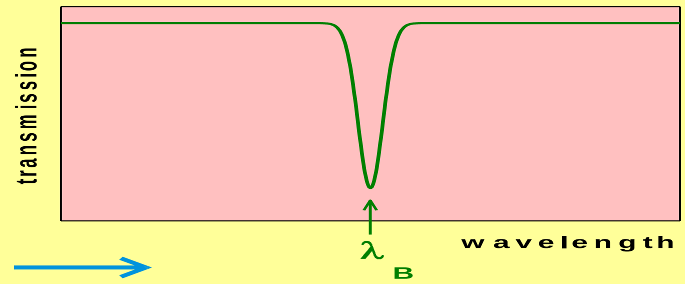

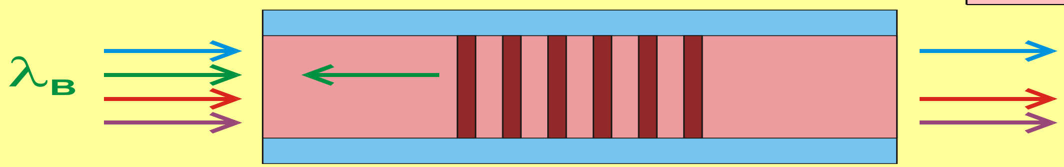

selectively reflected $\lambda_B = 2\, n_{eff}\, \Lambda$
reflectivity $R = \tanh^2 (k \times \Delta n \times L)$
$R<100\% \;\rightarrow\; \Delta\lambda \sim 0.1\text{nm}$ / $R>100\% \;\rightarrow\; \Delta\lambda$ broader

$\Rightarrow$ diverse applications based on selective separation of closely spaced λ 's

other types

variation of Λ, Δn_{mod}, phase front direction
multiple gratings, phase shift gratings

temperature and strain dependence

n and Λ = f (T, strain) $\rightarrow$ λ_B = f (T, strain)
☺ sensors $\leftrightarrow$ ☹ DWDM

Schematic experimental set-up for hologram and grating writing

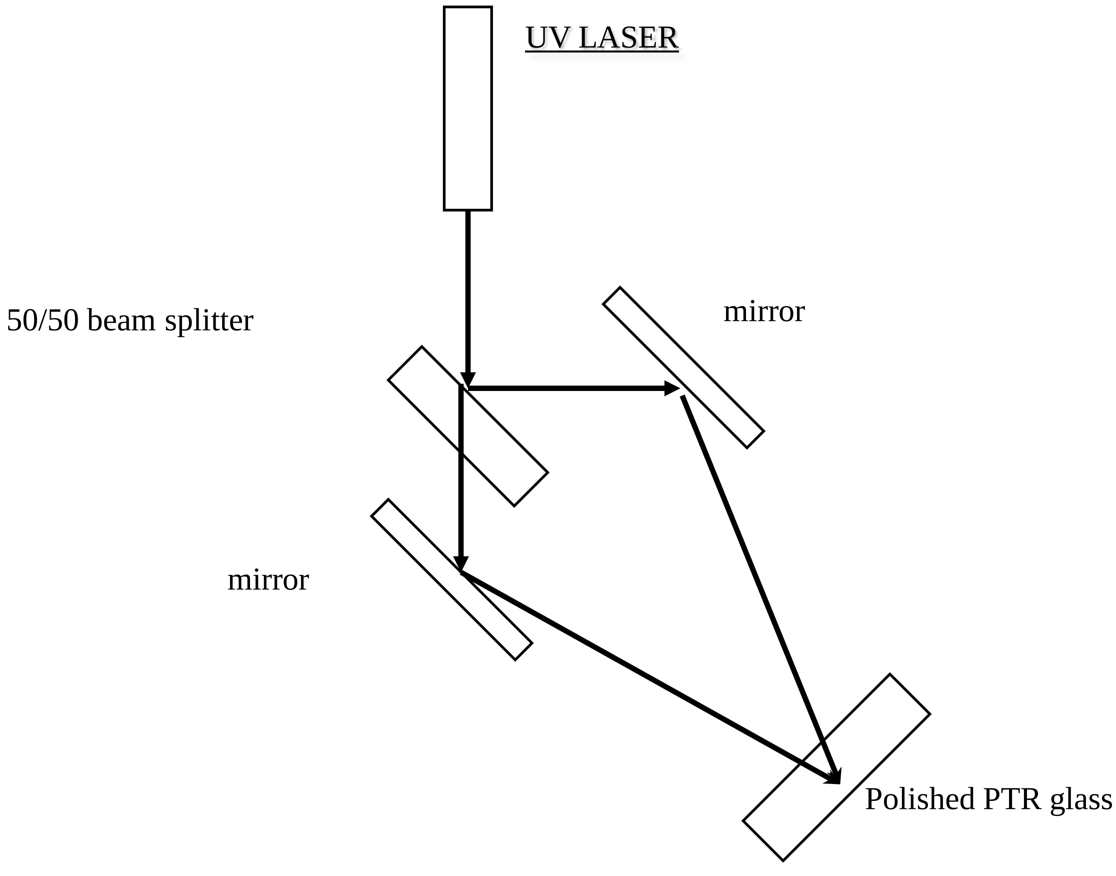

1D Gratings in planar devices

short device length

⬇

short grating length needed

⬇

high Δn required

e.g. R=95% $\rightarrow$ $\Delta n \cdot L = 1 \cdot 10^{-3}$ mm

	fiber	**planar**
Δn	$5 \cdot 10^{-5}$	$1 \cdot 10^{-3}$
L	2cm	1mm

Planar and volume Gratings

diffraction efficiency $\eta = I_R / I_0$

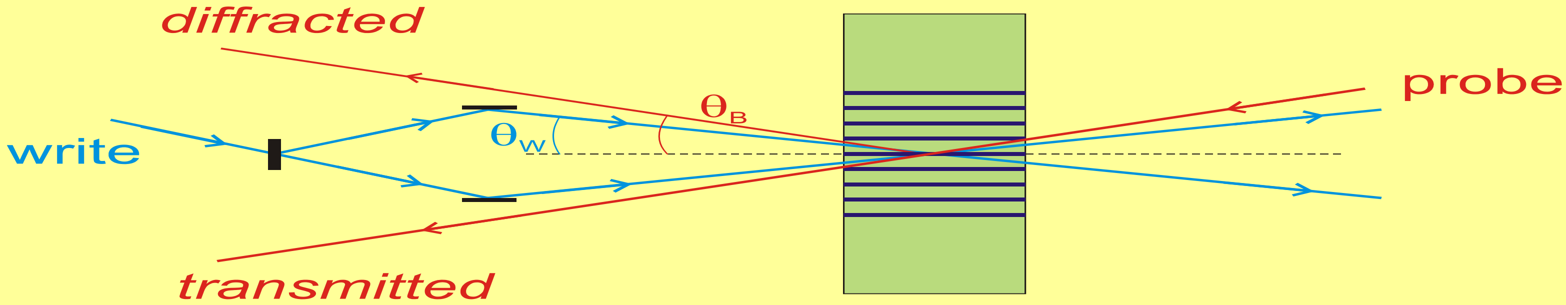

- **planar wave approximation:**
  $\eta = \sin^2 (\pi \cdot \Delta n \cdot L / \lambda_p / \cos \theta_B)$
  L = grating length $\rightarrow$ sample/film thickness

- **absorption in the sample**
  $\rightarrow$ effective thickness = $1 / \alpha_{laser}$
  $\rightarrow \Delta n(z) = n_0 \cdot \exp(-\alpha_{laser} \cdot z)$

f

lectured

Planar and volume Gratings

holographic information storage

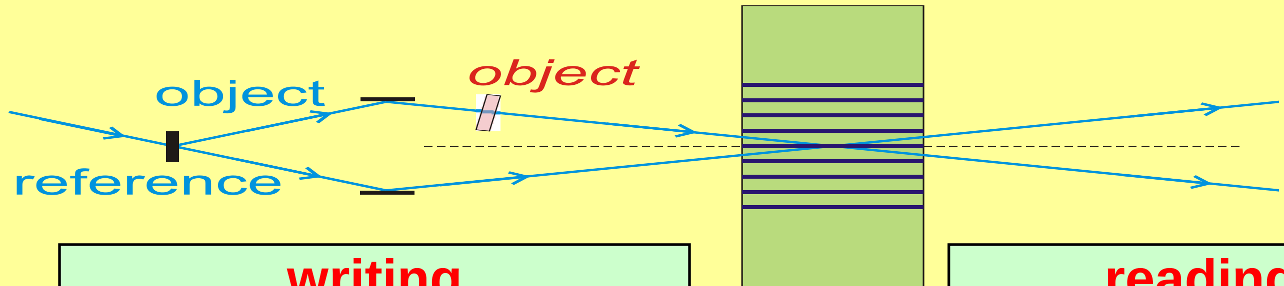

writing
object & reference
high power

reading
only reference
low power

advantages of glass:

- long-time storage
- room temperature operation
- multiple readings without degradation
  if $\lambda_w \neq \lambda_{peak}$ of Eu^{3+}

demultiplexing

- **frequency selective filters**
- **tuning by sample rotation and tilting**

$\rightarrow$ **different** $\theta_i \rightarrow$ **different** $\lambda_i = 2 \cdot \Lambda \cdot \sin\theta_i$

Fabrication of Waveguides

self-induced, self-written

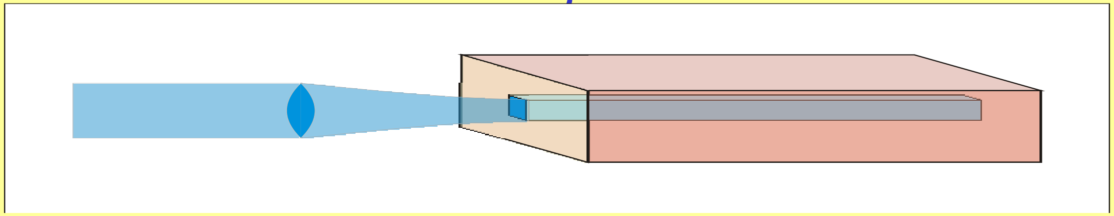

Direct write by sample translation

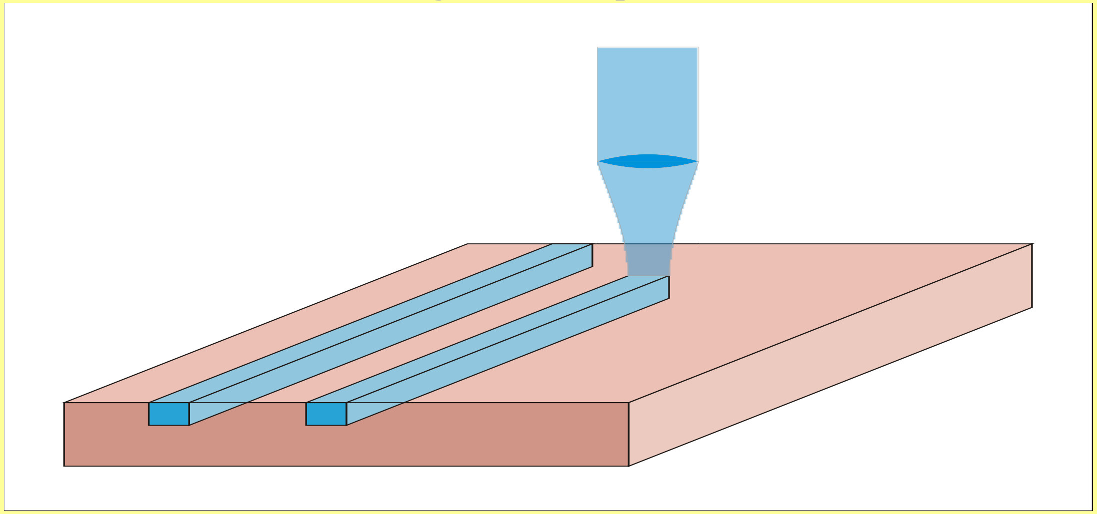

Waveguides

applications

fabrication of channel waveguides in integrated optical devices

- **easy and fast process**
- **no sharp bends $\rightarrow$ low rad. losses**

<u>self-writing:</u>

- **buried waveguides in one step**
- **complex structures (Y-couplers, tapers) by tailoring the writing beam shape**

waveguide characterization

- **waveguide image and mode-profile**
- **surface changes by AFM and profilometer**
- **Δn measurements:**

  from NA but modelling complex mode-profiles?

  from beam output narrowing during self-writing

Glasses for Waveguides

GaLaS, FP:Ce,Eu, PbO-SiO_2, Ge-SiO_2

- **244nm cw, direct-writing**

Na-borosilicate:Nd, Ge-SiO_2

- **455-488nm cw**
- **high transmission $\rightarrow$ self-writing**

oxide, fluoride, sulfide

- **800nm fs, train of pulses**

Material response: Direct-writing in fused silica
-tuning to absorption is only part of the issue

- Multi-photon exposure conditions
- 800 nm fs pulses; shown is dose
- Waveguide homogeneity highly dependent on irradiation parameters
- High pulse energy and/or slow translation speed induces too much inhomogeneity to support waveguiding
- Low pulse energy and/or fast translation speed results in not inducing a high enough Δn to support waveguiding

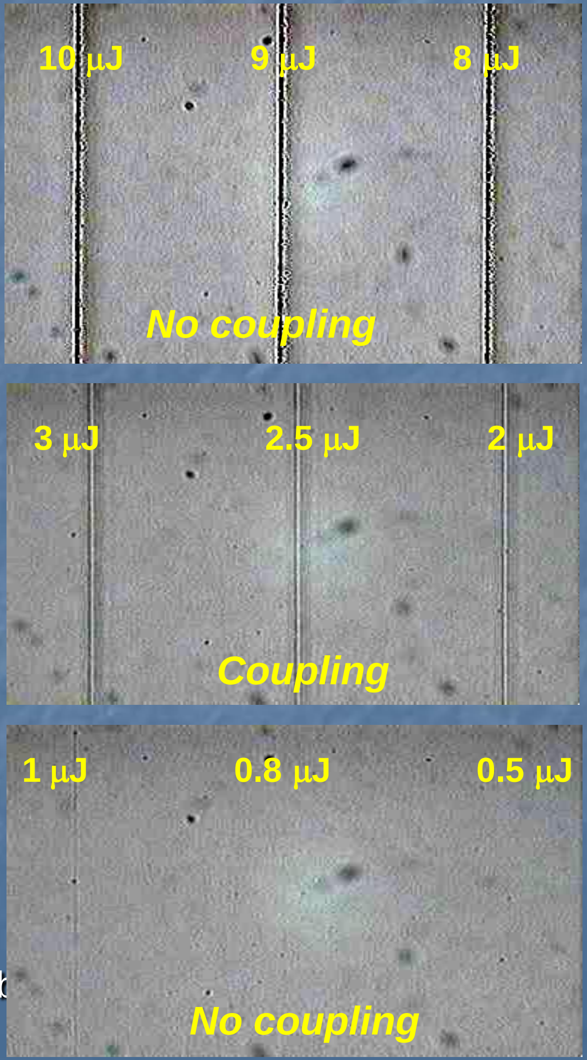

Direct-write in fused silica

- ***The resulting refractive index change is estimated from the waveguide NA***

$$NA = \sqrt{2n\Delta n}$$

$$\Delta n \cong \frac{n_1 - n_0}{n_1}$$

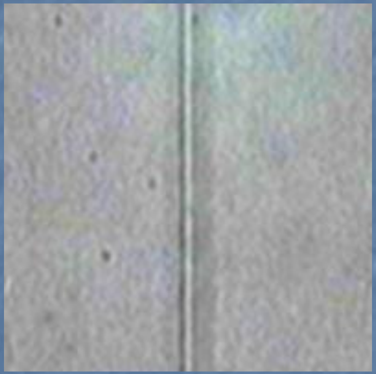

Cross-sectional view | Transverse view

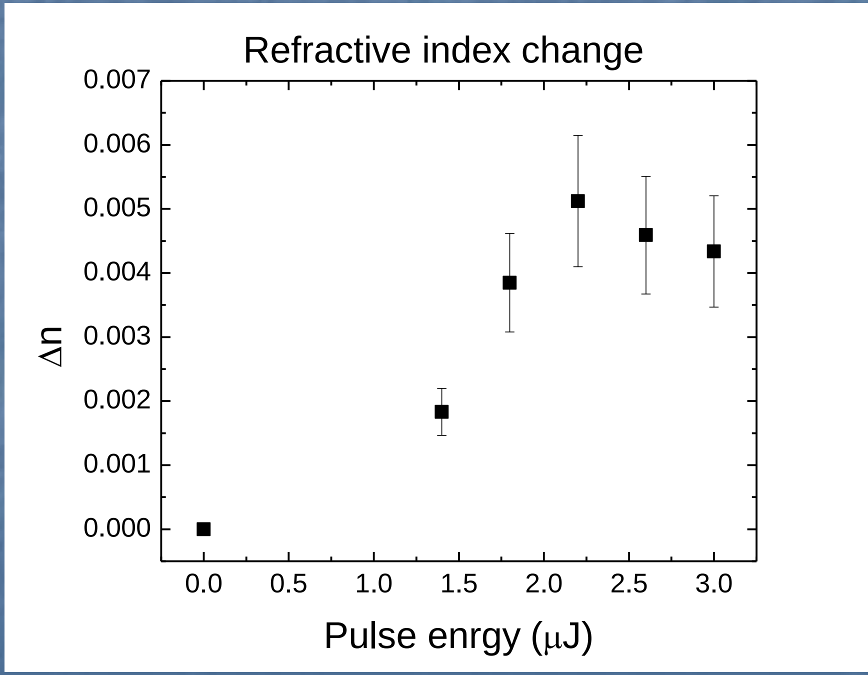

Typical $\Delta n \sim 0.004$
Pulse energies ~ few μJ

Direct-write in fused silica

- ***Different modes are supported depending on the Δn created***

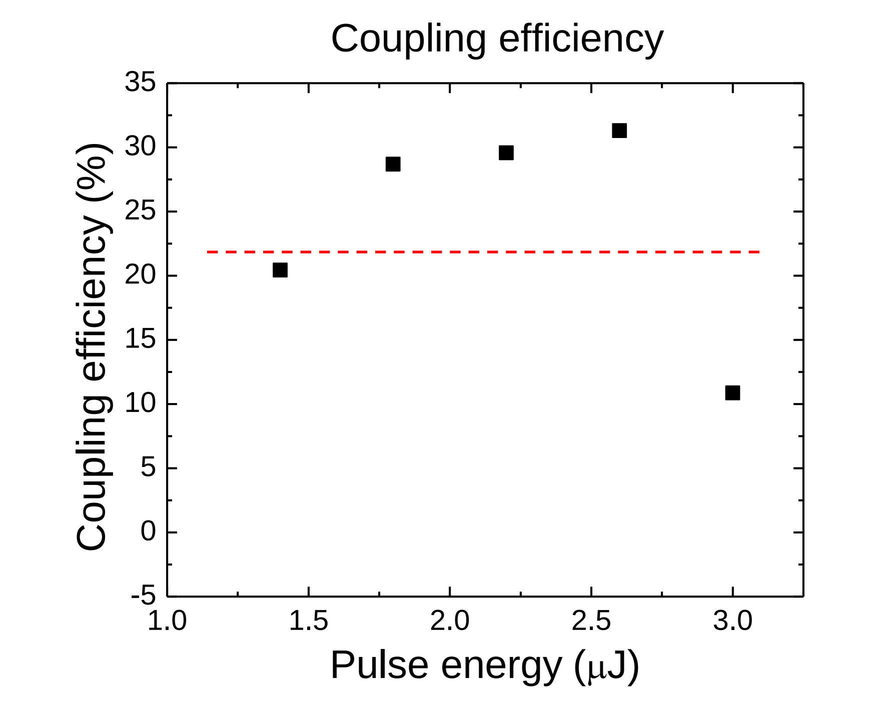

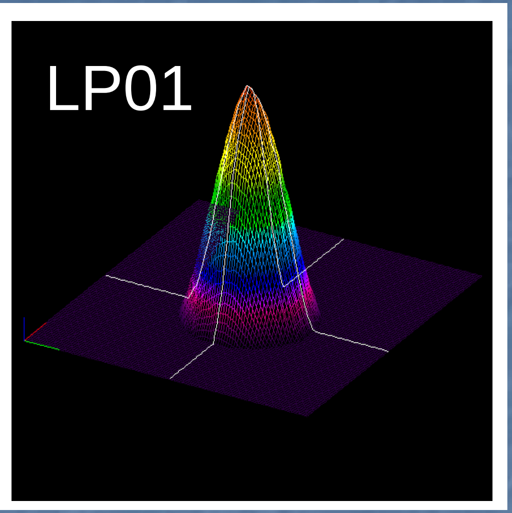

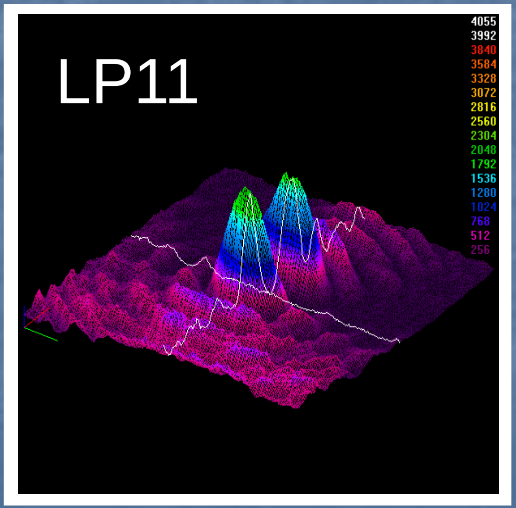

Coupling efficiency ~30%

Direct-write in IOG-1 (phosphate) glass - fs (130 fs)-written (800 nm), 0.3 μJ/pulse (D. Krol, UC-Davis/LLNL)

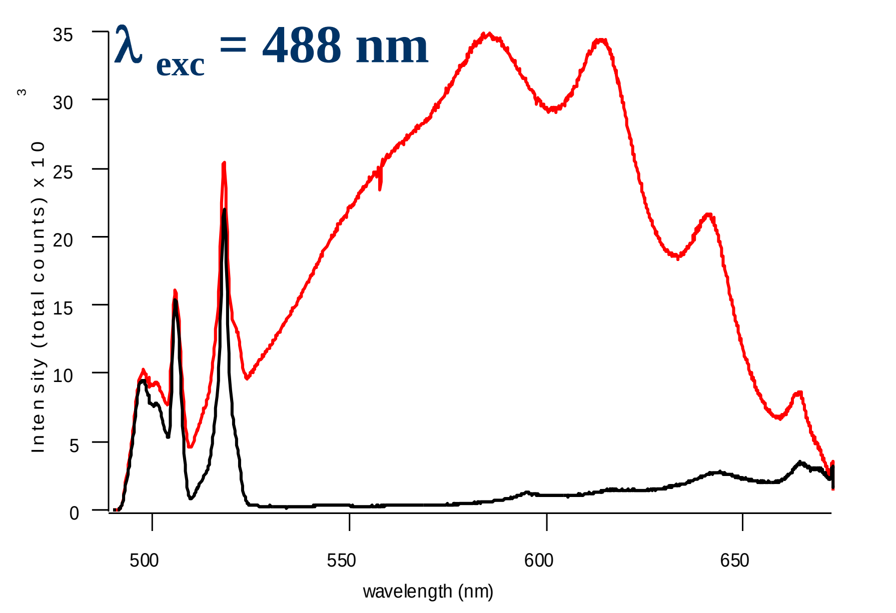

Fluorescence spectra (left) for modified (red) and unmodified (black) IOG-1 phosphate glass. λ_{exc} = 488 nm. Increase emission is attributable to formation of POHC defect upon illumination via proposed mechanism below.

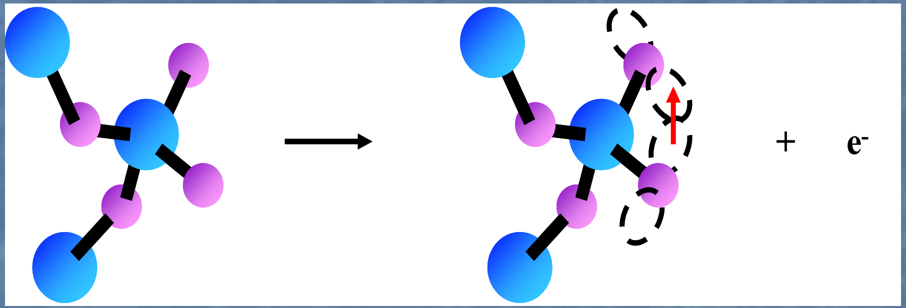

Proposed mechanism for the production of phosphorus-oxygen hole center (POHC) defects. The precursor consists of two non-bridging oxygen (NBO) atoms (pink) connected to a phosphorus (blue) atom, a defect that is common in phosphate glasses. A hole gets trapped on two orbitals of the two oxygen atoms to form the POHC. Resulting index change in exposed region of the glass is (-).

Absorption and *induced* absorption in ChG: influence of Se

- **Substitution of As atoms by chalcogens has little effect on linear absorption (in 3->7 series)**
- **Nonlinear absorption changes**
- **Se content primary α driver; not only participant for $\Delta\alpha$**

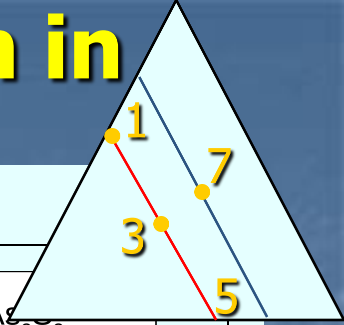

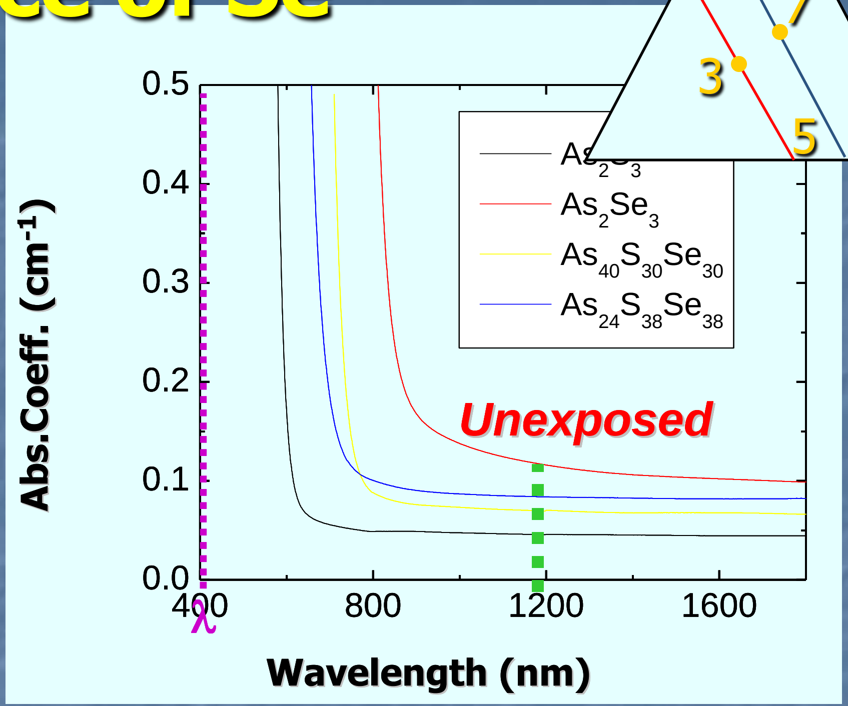

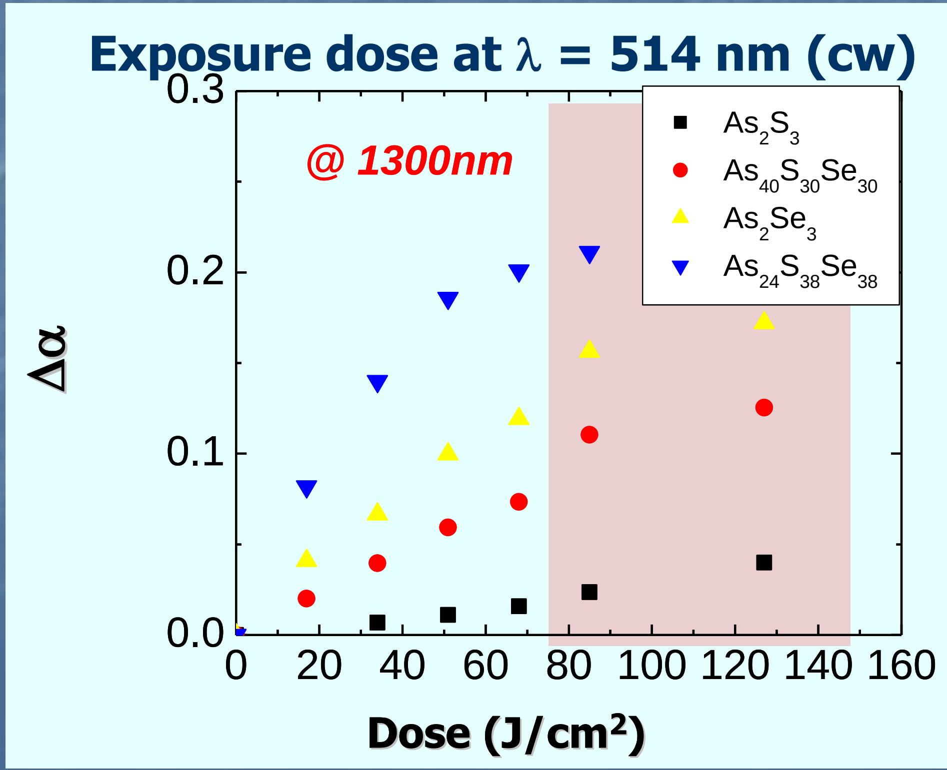

- **Extent of modification ($\Delta\alpha$) increases with dose; effect is directly related to chalcogen (primarily Se) content**
- **Not solely linear with chalcogen content; nonlinear absorption (two photon?)**
- **Influence of lone pair(s) of species affects n_2**

Photo-induced index change: Δn measurement in As_2S_3

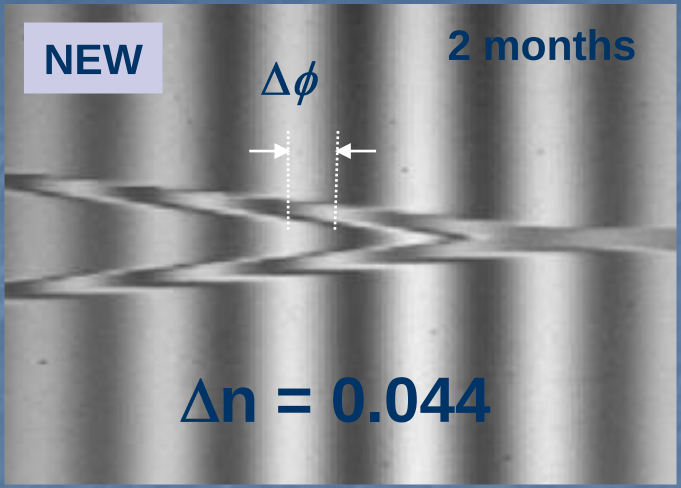

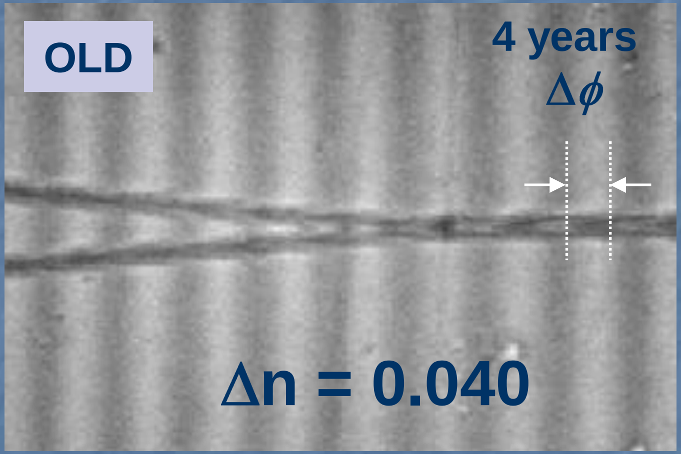

The Δn value relates to the measured phase shift $\Delta\phi$ by:

$$\frac{\Delta\phi}{2\pi} = \frac{2d}{\lambda}\Delta n$$

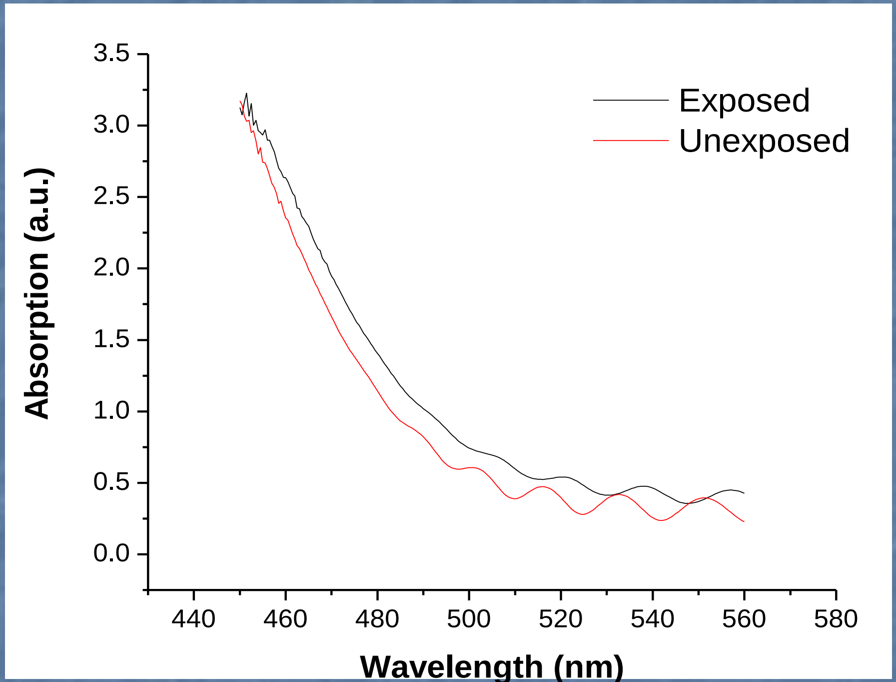

- **Aging to remove deposition-induced stress to yield stable, relaxed network structure *<u>does not adversely affect resulting film photosensitivity</u>*.**
- **Measured Δn is similar to those from early studies using short wavelength light**

Omachi et al., Appl Phys. Lett. (1972), $\Delta n = 0.104$
Petkov et al., J Non-Cryst. Sol, (1972), $\Delta n = 0.056$

Dose/Intensity-dependence on induced Δn (λ=800 nm, 100 fs pulses, 24 MHz rep rate): As_2S_3 films

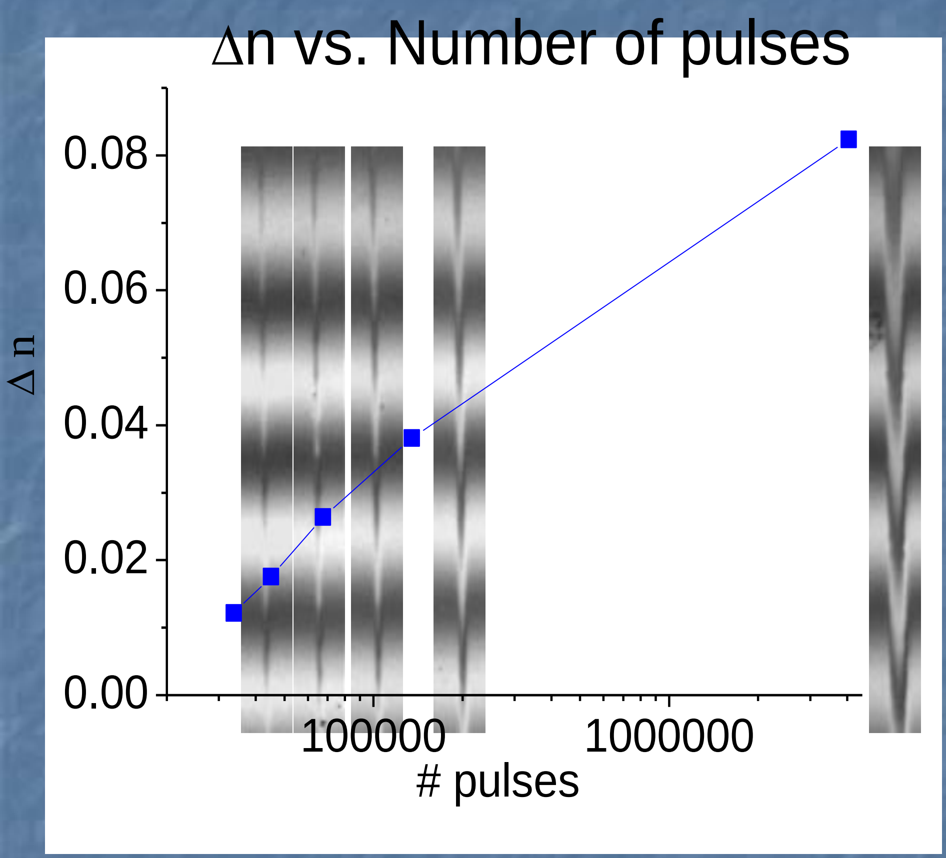

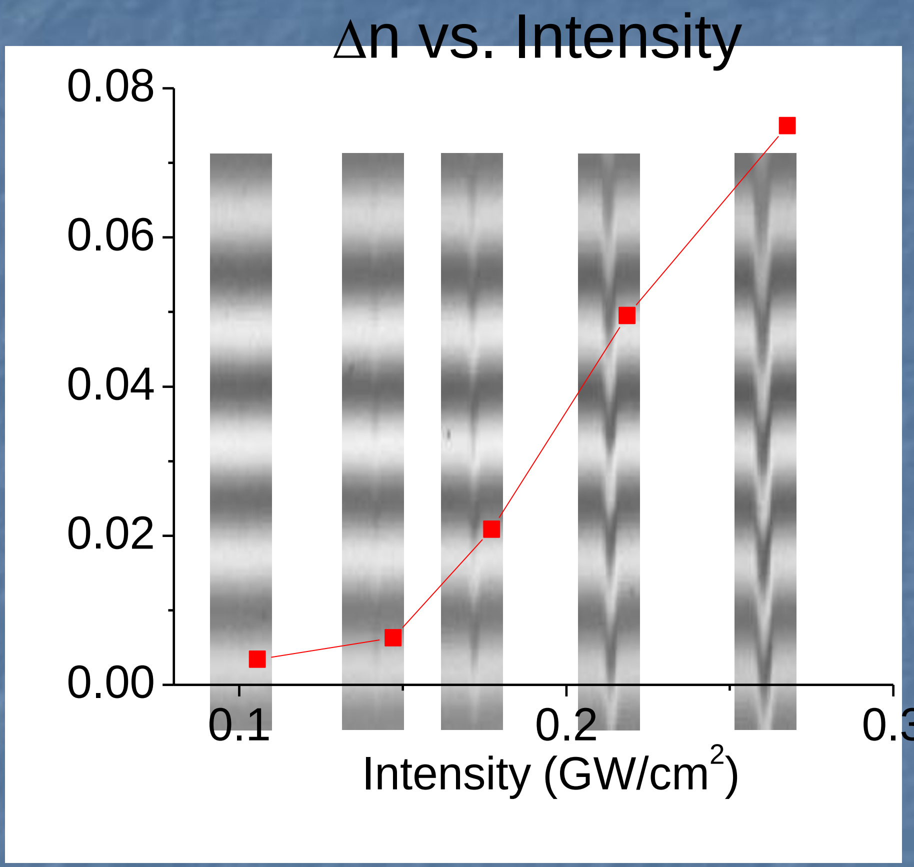

The Δn values measured for As_2S_3 (> 0.08) are much larger than for oxide glasses: saturation?

MHz fs laser machining system with in-situ microRaman spectroscopy

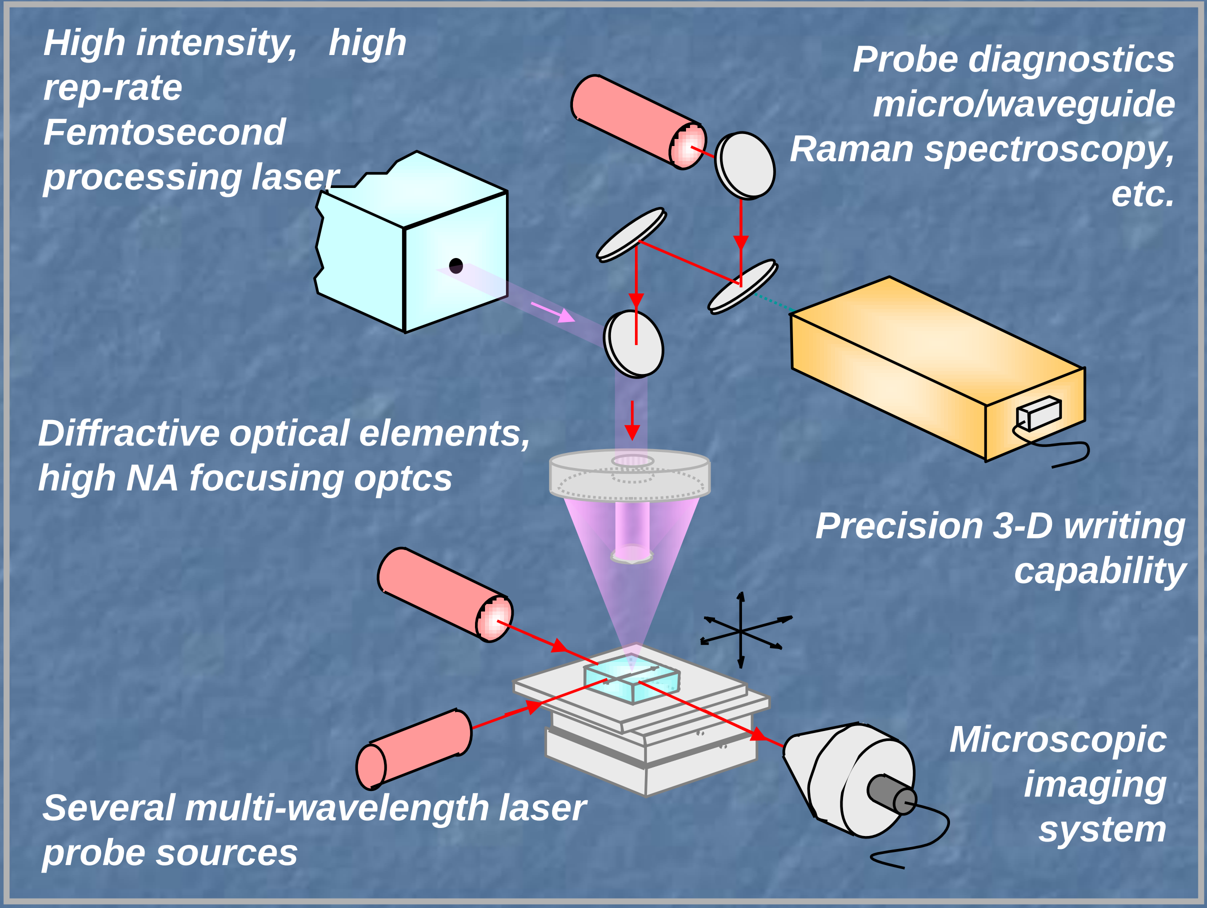

- **<u>Goal:</u> probe *dynamic* material response during laser writing to ascertain detailed knowledge of material modification mechanisms and kinetics**

Supported through NSF-MRI grant # DMR 0321110, "Development of a Femtosecond Laser-Materials Irradiation and In-Situ Probing Facility for Nano- and Micro-processing Applications and Student Training"

Free electron model in As_2S_3

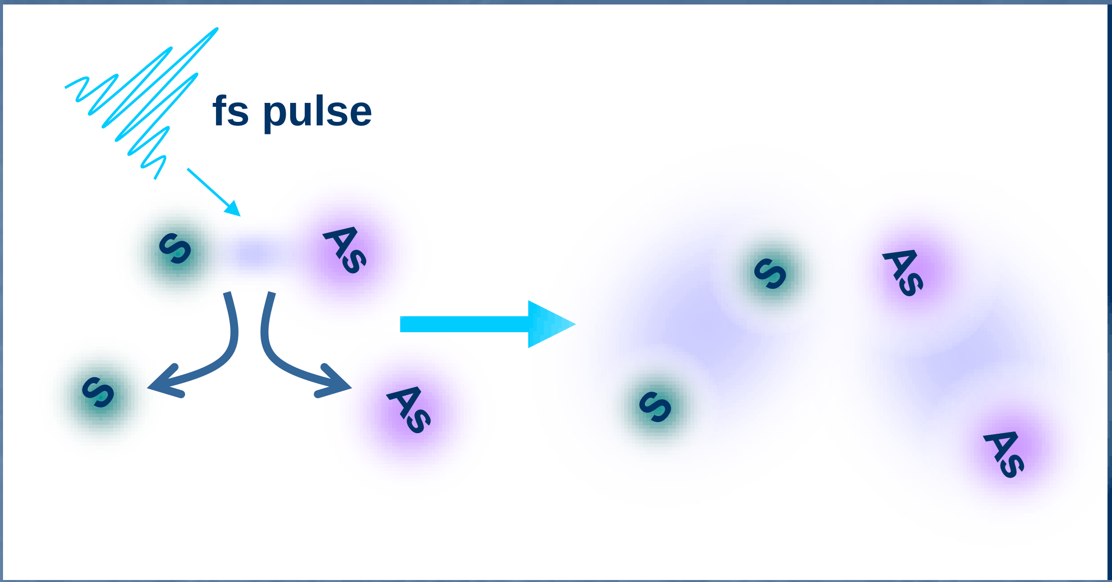

- *Photo-chemical: bond modification*
- *Photo-expansion: ΔV*
- *Photo-refraction: Δn*
- *Photo-darkening: $\Delta\alpha$*
- *Increase in thermal conductivity (via μTA): $\Delta\kappa$*

Avalanche ionization

$$\frac{\partial n_e}{\partial t} = \alpha I(t) n_e + \sigma_k I(t)^k$$

Multiphoton ionization

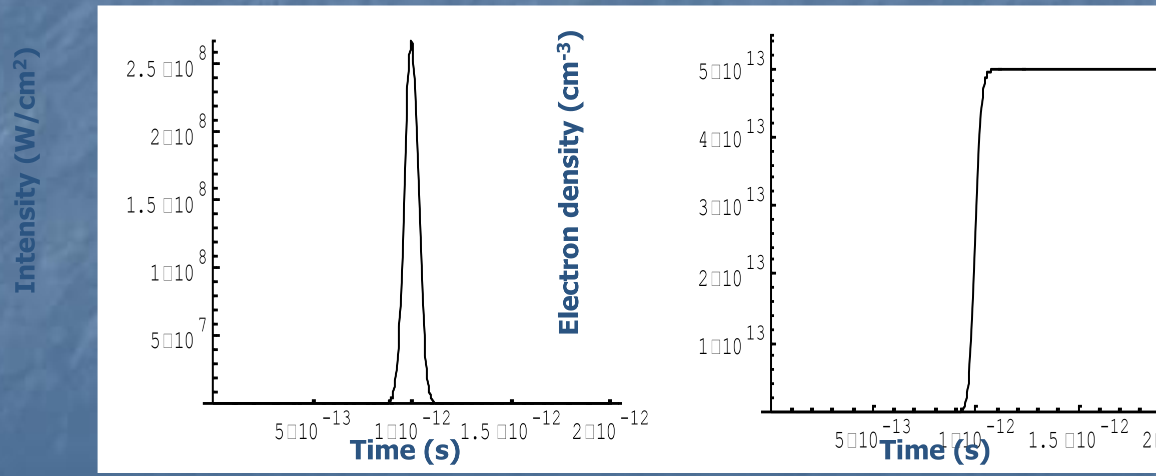

From Stuart, B.C. et al., JOSA B, Vol. 13, (1996) 459-468

A. Zoubir, et al., "Direct femtosecond laser writing of waveguides in As2S3 thin films," Optics Letters, Vol. 29 7 (2004) XXX

Free electron model

$$\frac{\partial n_e}{\partial t} = \sigma_k I(t)^k \cdot \frac{N_0 - n_e}{N_0}$$

Free electron density

<u>Depletion parameter</u>: maximum number of bonds available to participate in the photo-chemical reaction process

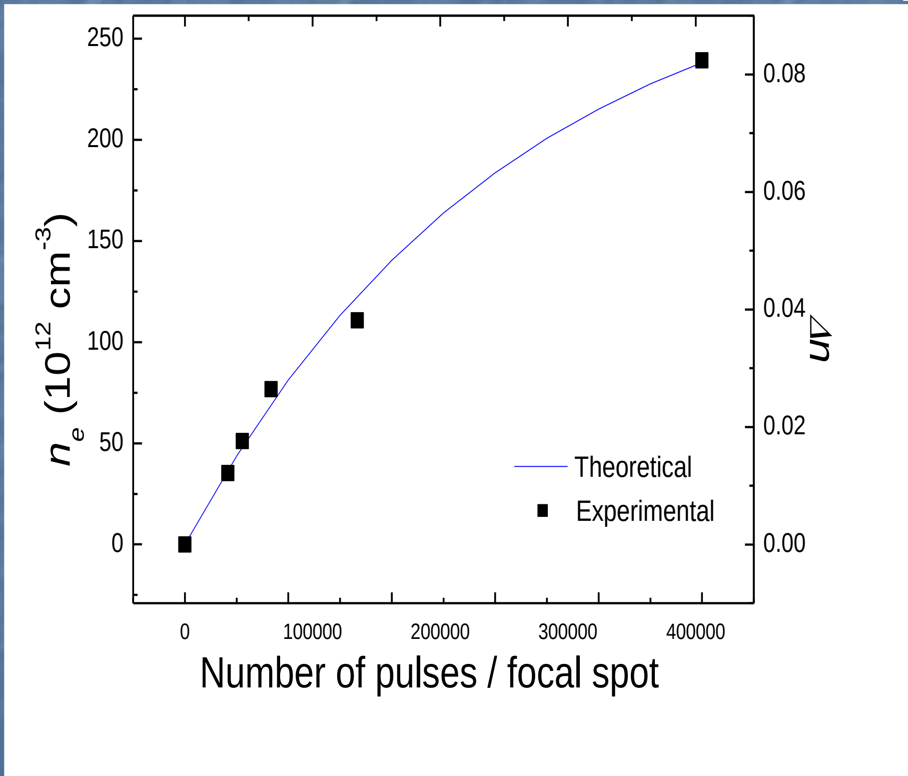

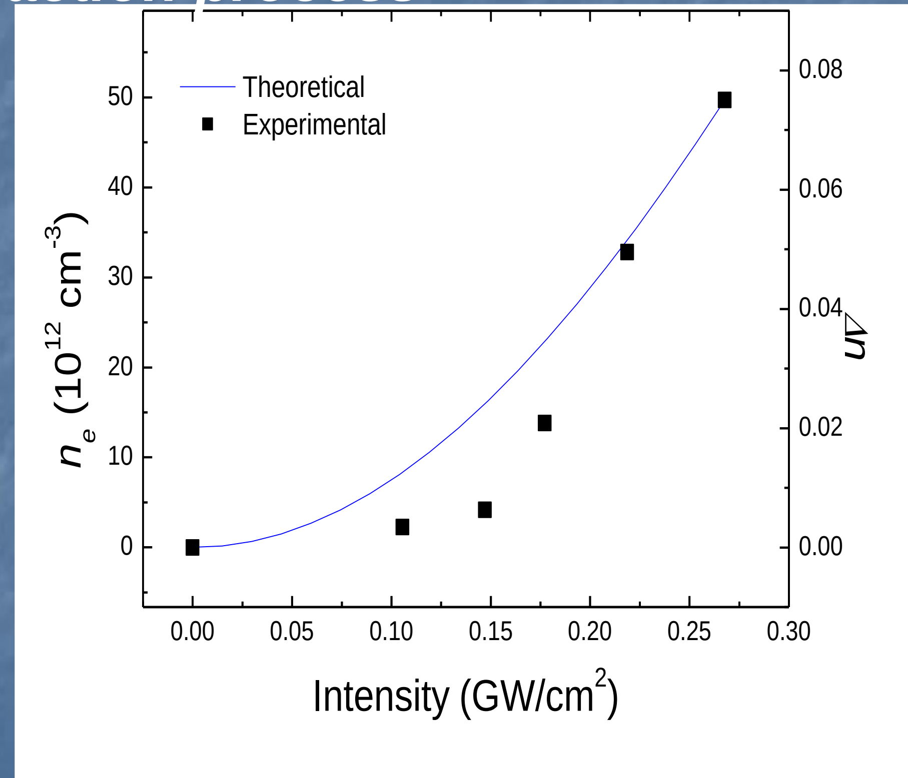

A. Zoubir et al., "Direct femtosecond laser writing of waveguides in As_2S_3 thin films" <u>Optics Letters</u> 29 7 (2004)

Direct write in polymers: absorption

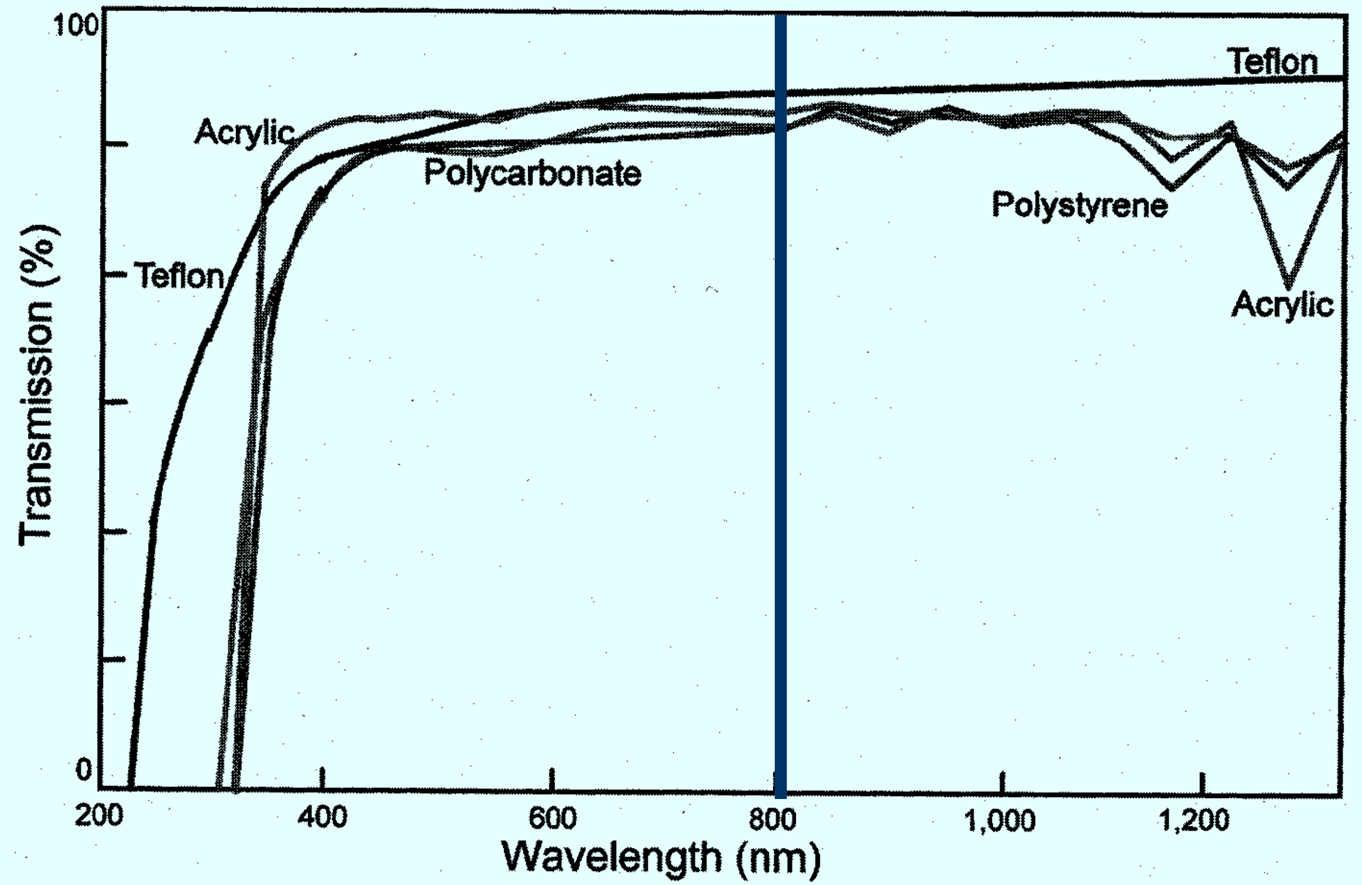

Figure 4.10: Transmission curves for a representative group of polymers. Loss in the IR comes from multiphonon absorption of light carbon-bonded species (C–H) (after Keyes 1995).

3-D writing in PMMA

fs writing (800 nm) in 25 MHz irradiation regime

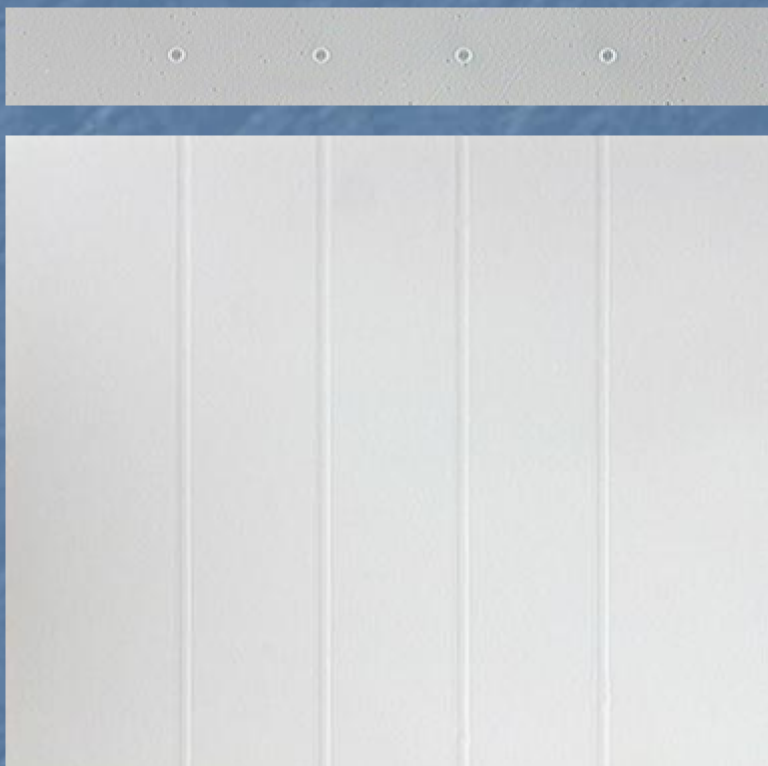

1-channel waveguides

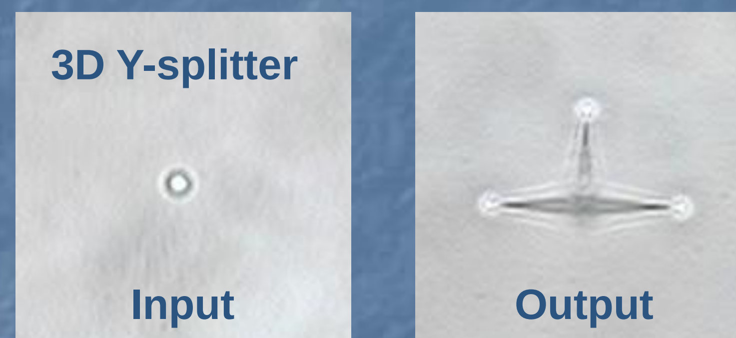

"Femtosecond laser fabrication of tubular waveguides in PMMA,"
A. Zoubir, C. Lopez, M. Richardson, K. Richardson, <u>Optics Letters,</u> in press, (2004)

Direct-write in PMMA

- **Low cost of production and ease of processing and fabrication**
- **Can be easily tailored to obtain the desired optical parameters (nonlinear coefficient, electro-optic coefficient, photosensitivity)**
- **Can be doped with conjugated chromophores or rare-earth ions**

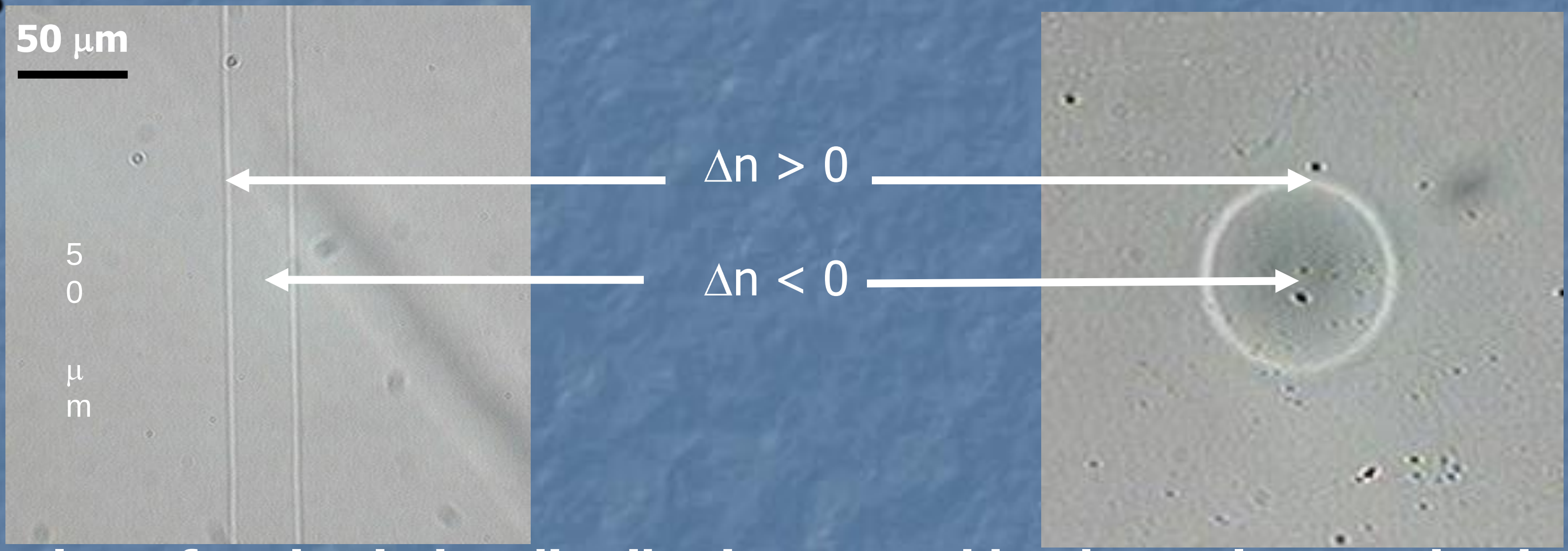

- **Annular refractive index distribution caused by thermal expansion in the focus - resolved by a DIC microscope**
- **(-) induced index is similar for other chain-structured materials such as in glass materials such as phosphate glass (Schott IOG-1)**

see "Chan et al., "Fluorescence Spectroscopy of Color Centers Generated in Phosphate Glasses after Exposure to Femtosecond Laser Pulses," 85 5 1037 (2002)

Direct-write in PMMA

Structures are highly multi-mode (large dimensions)

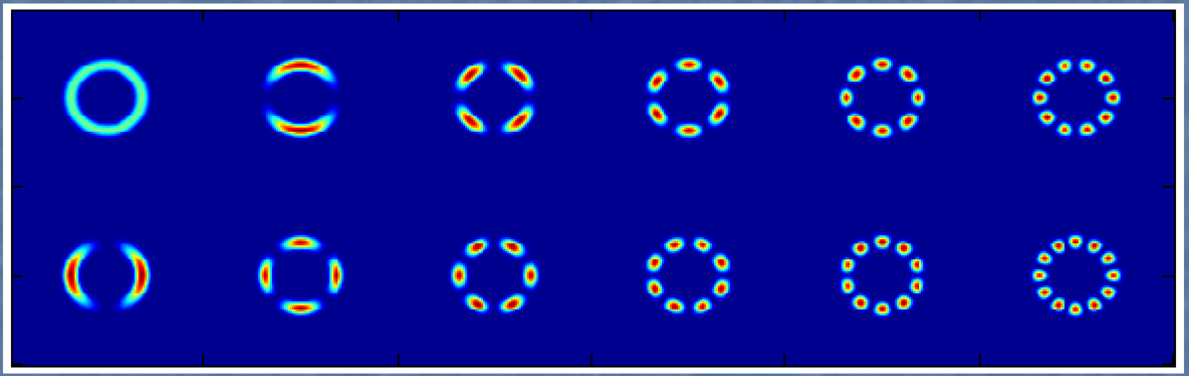

Unusual mode are allowed to propagated in such structures

- ***Near-field intensity distribution measured and calculated by the finite-difference method***

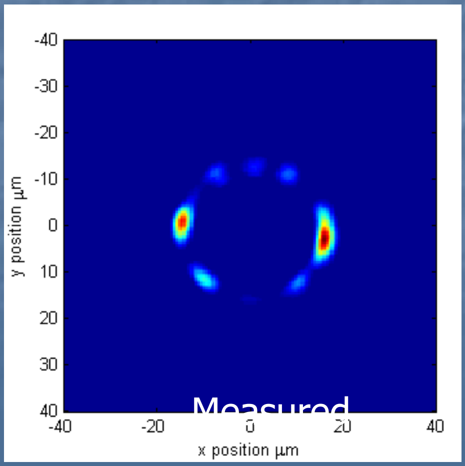

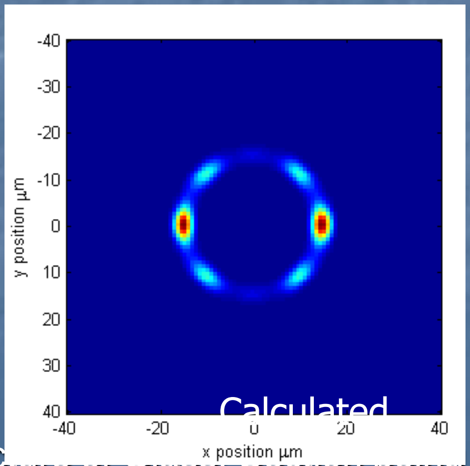

Refractive index change estimated from simulation: $\Delta n \sim 0.002$